

AN ADAPTIVE N-PATH FILTER

by

WALTER EDWARD GRANBERRY, JR. B.S. in E.E.

A THESIS

IN

ELECTRICAL ENGINEERING

Submitted to the Graduate Faculty
of Texas Tech University in
Partial Fulfillment of
the Requirements for
the Degree of

MASTER OF SCIENCE

IN

ELECTRICAL ENGINEERING

Approved

Accepted

December, 1976

AC
805

TZ
1976

No. 151

COO.2

ACKNOWLEDGMENTS

I am deeply indebted to Professor R. H. Seacat for his support and guidance during my studies at Texas Tech. I am also grateful to Dr. T. R. Burkes and Dr. J. P. Craig for their many contributions to the development of this thesis.

TABLE OF CONTENTS

ACKNOWLEDGMENTS	ii
LIST OF FIGURES	v
I. INTRODUCTION	1
II. THE N-PATH FILTER	4
A. A General Input-Output Relation for the N-Path Filter	4
B. System Function Characterization of the N-Path Filter	10
C. A System Function for the Case of Binary Modulating Functions	11
D. A System Function for Frequency-Modulated Signals	18
E. Noise Bandwidth of the N-Path Filter	22
F. Obtaining Modulating Functions for the N-Path Filter	25
III. DESIGN AND EXPERIMENTAL DEMONSTRATION OF AN ADAPTIVE N-PATH FILTER	29
A. Design of the N-Path Filter	29
B. The Phase-Locked Loop and Decoding Network	33
C. Signal Sources Used in the Filter Evaluation	36
D. Experimental Measurements	36
E. Magnitude-Frequency Characteristics of the N-Path Filter, Sinusoidal Inputs	38
F. Adaptive Filtering of Noisy Signals, Externally Supplied Reference Frequency	40
G. Adaptive Filtering of Noisy, Frequency- Modulated Signals, Reference Derived from the Filter Output	43

IV. CONCLUSIONS	50
LIST OF REFERENCES	53
APPENDIX A	54
APPENDIX B	57

LIST OF FIGURES

2.1	An N-path filter	6
2.2	N-path network characterized by a system function	12
2.3	Modulating functions $p_n(t)$ produced by periodic switching	14
2.4	Plot of $ T(j\omega) $ vs ω for N-path filter with $N = 8$	16
2.5	Block diagram of elementary phase-locked loop and decoding network	27
3.1	Block diagram of the adaptive N-path filter	30
3.2	Block diagram of the eight-section filter	33
3.3	Phase-locked loop and decoding network	34
3.4	Signal Sources used in the N-path filter system filter measurements	37
3.5	Magnitude-frequency plot of N-path filter system function, unmodulated case	39
3.6	Magnitude-frequency plot of $ T(j\omega) $ showing "comb filter" response	41
3.7	Magnitude-frequency plot of N-path filter system function, frequency-modulated case	42
3.8	Sine wave filtered from wide-band noise, signal amplitude 10 mV p-p, noise 2.5 V RMS	44
3.9	Triangular wave filtered from wide-band noise, signal amplitude 10 mV p-p, noise 2.5V RMS	45
3.10	Square wave filtered from wide-band noise, signal amplitude 10 mV p-p, noise 2.5 V RMS	45
3.11	Pulses filtered from wide-band noise, signal amplitude 10 mV p-p, noise 2.5 V RMS	45

3.12	Frequency-modulated sine wave filtered from wide-band noise, signal amplitude 200 mV p-p, noise 2.5 V RMS	47
3.13.	Maximum modulating frequency f_s as a function of input signal/noise ratio, signal amplitude 200 mV p-p	48

CHAPTER I

INTRODUCTION

Determining the presence of a signal embedded in wide-band noise requires systematically searching through frequency (and often time) for energy that is not noise-like. Once a signal or signal components are identified from the noise, the signal may be recovered by means of frequency-domain filtering. Frequency-domain filtering may be accomplished by digital or analog methods. Digital techniques frequently employ real-time Fourier or Walsh transform algorithms to break the signal into orthogonal functions which can be represented in the frequency domain. Filtering is accomplished by inverse transforming cells in the frequency domain which are assumed to contain the signal and have significantly more energy than surrounding cells. Both adaptive and non-adaptive digital filtering techniques have been successfully applied to the recovery of signals from wide-band noise, but the required hardware is very complex and generally expensive.

An adaptive analog filter is the subject of this thesis. This filter, called an "N-path filter", can be used for increasing the signal/noise ratio by passing energy at frequencies coinciding with significant components of the signal spectrum, while rejecting energy at other frequencies. Such a filter may act as a kind of matched

filter for signals which may be frequency or phase-modulated, and which may be subject to oscillator drift or Doppler shift. Possible applications of the filter include recovery of periodic band-limited signals from noise, phase-locked loop threshold extension, and measurement of very low signal/noise power ratios.

In succeeding chapters the N-path filter which can, under certain conditions, generate a transfer function characterized by a sequence of narrow band-pass regions will be described. The number and center frequency of these band-pass regions are determined by the filter and the frequency spectrum of modulating functions supplied to the filter from an external source. The modulating functions may be derived from the signal which is being filtered by means of a phase-locked loop. Under these conditions, the adaptive filter and phase-locked loop may act as a low-threshold receiver-demodulator.

An analysis of an elementary phase-locked loop will be developed. A linearized model is derived and is analyzed to determine the noise bandwidth of the loop. The analysis is extended to determine the effect of the preceding N-path filter upon the loop noise bandwidth. The loop noise bandwidth may be calculated using loop parameters, and may be used to predict the signal/noise ratio inside the loop which results from a known

signal/noise ratio at the loop input.

After the analytical and design techniques have been developed, the hardware realization of an N-path filter and a phase-locked loop modulating function generator, using standard integrated circuits, will be described. The experimental system, including the noise source, will also be discussed.

The hardware realized by these techniques has been tested. Data taken on the filter system will be presented for noise-free and low signal/noise ratio operation, in both fixed-frequency and frequency-modulated cases. Concluding remarks will be made concerning the filter system and possible improvements which may be made. Several areas for further investigation of the system will also be discussed.

CHAPTER II

THE N-PATH FILTER

A time-varying R-C network which, under certain conditions, may be characterized by a system function has been described in the literature [1]. Termed an "N-path filter", the network consists of low-pass filters and analog multipliers, as shown in Figure 2.1.

The modulating functions $p(t)$ and $q(t)$ are synchronized to the input, $u(t)$. The low-pass filters, having identical impulse response, $h(t)$, will charge to some average voltage $y(t)$. This voltage is transferred to the output through the output multipliers and a summing point. Depending upon the type of modulating functions and low-pass filters which are used, a number of interesting input-output relationships will be produced. A general input-output relationship for the filter of Figure 2.1 has been derived by Franks and Sandberg, and the analysis herein uses much of the original notation [2].

A General Input-Output Relation for the N-Path Filter

Consider the N-path network of Figure 2.1. The input multipliers operate on the input $u(t)$ to produce the inputs $x_n(t)$ to the low-pass filters such that

$$x_n(t) = u(t)p[t - (n - 1)\tau]. \quad (2.1)$$

Each of the N outputs $y_n(t)$ which are obtained from the

low-pass filters are multiplied by the corresponding output modulating functions and are summed to form the output $v(t)$. The input and output modulating functions, $p[t-(n-1)\tau]$ and $q[t-(n-1)\tau]$ respectively, are assumed periodic with the period $T = N\tau$ in this analysis. The modulating functions can be expanded in a Fourier series as

$$p(t) = \sum_{m=-\infty}^{m=\infty} P_m e^{j\omega_0 m t} \quad (2.2)$$

and

$$q(t) = \sum_{\ell=-\infty}^{\ell=\infty} Q_\ell e^{j\omega_0 \ell t}, \quad (2.3)$$

where

$$\omega_0 = 2\pi/T = 2\pi/N\tau. \quad (2.4)$$

Let us define

$$p_n(t) = p[t-(n-1)\tau], \quad (2.5)$$

and

$$q_n(t) = q[t-(n-1)\tau]. \quad (2.6)$$

The Laplace transforms of $p_n(t)$ and $q_n(t)$ will be denoted $P_n(s)$ and $Q_n(s)$ respectively. Each term in the series given by (2.2) and (2.3) is of the general form

$$f_k(t) = \sum_k c_k e^{a_k t}. \quad (2.7)$$

Because Laplace transform expressions and convolutions

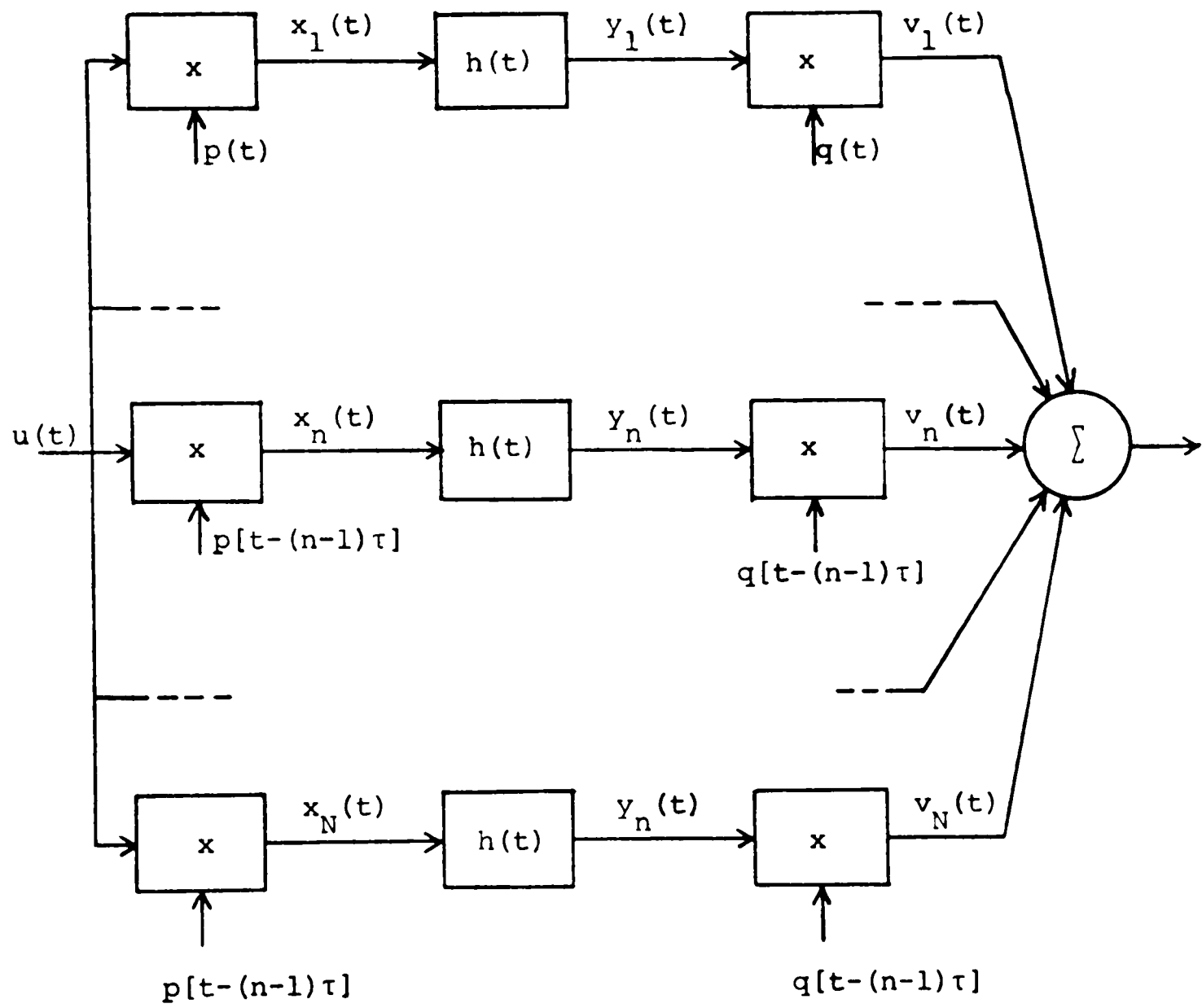


Figure 2.1. An N-path filter.

containing terms of this form will appear in the derivations which follow, it is necessary to examine several relations which will be used in the derivations. Applying the relation at
 $L[e^{at}] = 1/(s-a)$, it is evident that

$$L[f_k(t)] = \sum_k c_k / (s-a_k) \quad . \quad (2.8)$$

Also

$$L[e^{bt}g(t)] = G(s-b), \quad (2.9)$$

where $G(s) = L[g(t)]$.

Now assume that all of the time functions associated with the N-path filter are Laplace transformable. The Laplace transform representation of the output of the filter $V(s)$ may be written in terms of the functions which are multiplied by the output multipliers as follows:

$$V(s) = \sum_{n=1}^{n=N} V_n(s) = \sum_{n=1}^{n=N} L\{y_n(t)q_n(t)\}. \quad (2.10)$$

Expressing $q_n(t)$ by a Fourier series, substituting into (2.10), and applying (2.9) to the result yields

$$\begin{aligned} V(s) &= \sum_{n=1}^{n=N} L\{y_n(t) \sum_{\ell=-\infty}^{\infty} Q_{\ell} e^{j\omega_0 \ell [t-(n-1)\tau]}\} \\ &= \sum_{n=1}^{n=N} \sum_{\ell=-\infty}^{\infty} Q_{\ell} e^{-j\omega_0 \ell (n-1)\tau} Y_n(s-j\ell\omega_0). \end{aligned} \quad (2.11)$$

Referring to Figure 2.1, $y_n(s)$ can be written as

$$Y_n(s) = X_n(s)H(s); \quad (2.12)$$

hence (2.11) may be written in the form

$$V(s) = \sum_{n=1}^{n=N} \sum_{\ell=-\infty}^{\ell=\infty} Q_{\ell} e^{-j\omega_0 \ell (n-1)\tau} X_n(s-j\ell\omega_0)H(s-j\ell\omega_0). \quad (2.13)$$

Now referring to Fig. 2.1, $X_n(s)$ can be written as

$$X_n(s) = L\{u(t)p_n(t)\}. \quad (2.14)$$

The Fourier series of $p_n(t)$ may be substituted into (2.14), giving

$$\begin{aligned} X_n(s) &= L\{u(t) \sum_{m=-\infty}^{m=\infty} P_m e^{j\omega_0 m [t - (n-1)\tau]}\} \\ &= \sum_{m=-\infty}^{m=\infty} P_m e^{-j\omega_0 m (n-1)\tau} U(s-jm\omega_0). \end{aligned} \quad (2.15)$$

The term $X_n(s-j\ell\omega_0)$ which appears in (2.13) can be obtained from (2.15) by substituting $s-j\ell\omega_0$ for s , yielding

$$X_n(s-j\ell\omega_0) = \sum_{m=-\infty}^{m=\infty} P_m e^{-j\omega_0 m (n-1)\tau} U[s-j(m+\ell)\omega_0]. \quad (2.16)$$

Upon substitution of (2.16) into (2.13), the output of the filter may be written as

$$V(s) = \sum_{\ell=-\infty}^{\ell=\infty} \sum_{m=-\infty}^{m=\infty} \sum_{n=1}^{n=N} Q_{\ell} P_m e^{-j\omega_0 (m+\ell)(n-1)\tau} F(s, m) \quad (2.17)$$

where $F(s, m) = H(s-j\ell\omega_0)U[s-j(m+\ell)\omega_0]$.

The summation over n in (2.17) may be written as

$$\sum_{n=1}^N e^{-j\omega_0(m+l)(n-1)\tau} = \sum_{n=1}^N e^{-j\frac{2\pi}{N}(m+l)(n-1)}$$

where $\omega_0 = 2\pi/T = 2\pi/N\tau$.

Whenever $(m+l) = kN$, the series reduces to

$$\sum_{n=1}^N e^{-j2\pi k(n-1)} = N, \quad k = 0, 1, 2, \dots .$$

For $(l+m) \neq kN$, the summation is zero. Hence the summation can be written as

$$\sum_{n=1}^N e^{-j\omega_0(m+l)(n-1)\tau} = \begin{cases} N, & l+m = kN \\ 0, & \text{otherwise} \end{cases} . \quad (2.18)$$

Substituting (2.18) into (2.17) with $(l+m) = kN$, yields

$$V(s) = N \sum_{k=-\infty}^{\infty} \sum_{\ell=-\infty}^{\infty} Q_{\ell} P_{kN-\ell} H(s-j\ell\omega_0) U(s-jkN\omega_0), \quad (2.19)$$

which can be written in the form

$$V(s) = \sum_{k=-\infty}^{\infty} F(k,s) U(s-jkN\omega_0), \quad (2.20)$$

where

$$F(k,s) = \sum_{\ell=-\infty}^{\infty} N Q_{\ell} P_{kN-\ell} H(s-j\ell\omega_0) . \quad (2.21)$$

Equations (2.20) and (2.21) characterize the input-output relationship of the N -path network. The term $F(k,s)$ which

appears in (2.21), describes the specific operational link between the input and output signals, and is somewhat similar to a system function for a time-invariant network.

System Function Characterization of the N-path Filter

If the input and output signals of the N-path filter are band-limited, a system function representation of the filter can be easily found. In general it is necessary to filter the input and output signals with additional low-pass filters to force the signals $u(t)$ and $v(t)$ to be band-limited.

Assume such a band-limited input, where the input $U(s)$ evaluated on the $j\omega$ axis essentially vanishes for frequencies above $\frac{N}{2}\omega_0$ radians/second, that is, outside the interval $|\omega| < \frac{N}{2}\omega_0$. If indeed the output, $V(j\omega)$, vanishes outside the interval $|\omega| < \frac{N}{2}\omega_0$, or is forced to vanish by passing it through an ideal low-pass filter with cutoff frequency of $\frac{N}{2}\omega_0$ radians/second, the following relation may be written:

$$V(j\omega) = F(0, j\omega)U(j\omega) \text{ in the interval } |\omega| < \frac{N}{2}\omega_0, \quad (2.22)$$

where $F(0, j\omega) = F(k, s) \Big|_{s=j\omega}^{k=0}$.

The only allowed value of k is $k = 0$, since values of k greater than zero produce terms in $F(k, j\omega)$ corresponding to frequencies outside the interval $|\omega| < \frac{N}{2}\omega_0$. Because of

constraint that the input and output signals be band-limited, a new system function can be defined as follows:

$$V(j\omega) = T(j\omega)U(j\omega) , \quad (2.23)$$

where

$$T(j\omega) = \begin{cases} F(0, j\omega), & \text{in } |\omega| < \frac{N}{2}\omega_0 \\ 0, & \text{otherwise} \end{cases} . \quad (2.24)$$

From (2.21), the value of $F(k, s) \Big|_{\substack{k=0 \\ s=j\omega}}$ is

substituted into (2.24) to yield

$$T(j\omega) = \begin{cases} N \sum_{\ell=-\infty}^{\ell=\infty} P_{-\ell} Q_{\ell} H(j\omega - j\ell\omega_0), & |\omega| < \frac{N}{2}\omega_0 \\ 0, & \text{otherwise} \end{cases} . \quad (2.25)$$

The band-limiting constraint in (2.25) will be satisfied if ideal low-pass filters with cutoff frequency $\frac{N}{2}\omega_0$ radians/second are placed before and after the N-path filter. The system which results can be characterized by the system function $T(j\omega)$ in (2.25), as shown symbolically in Fig. 2.2.

A System Function for the Case of Binary Modulating Functions

The N-path network of Fig. 2.1 may be easily mechanized by using switches to replace the analog multipliers. This corresponds to binary modulating functions, which have a value of 0 or 1. Suppose that the modulating function $p(t)$ is a train of rectangular pulses

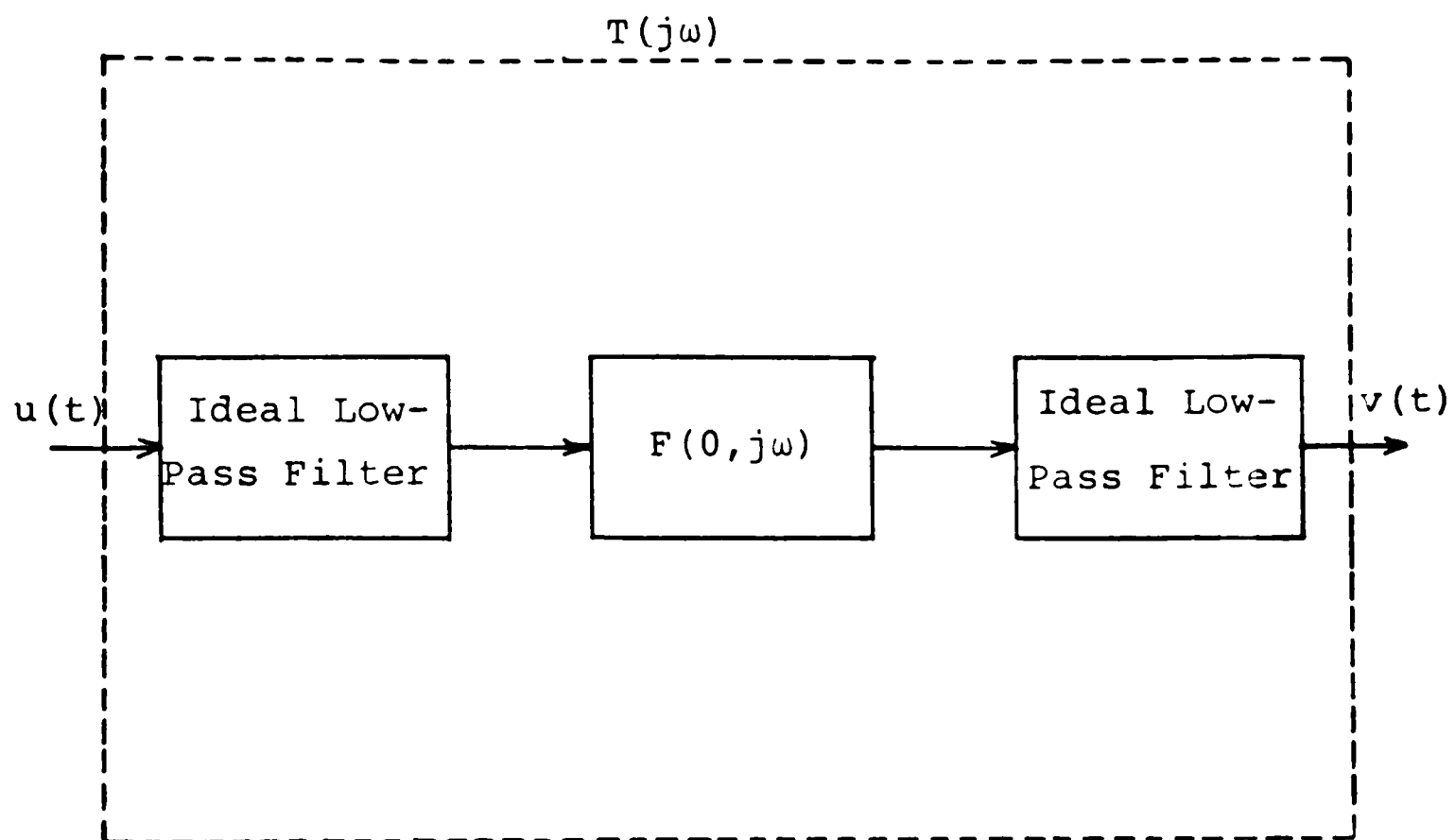


Figure 2.2. N-path network characterized by a system function.

having unity amplitude, period T , and width $\tau = T/N$, as shown in Fig. 2.3. This modulating function can be represented by the Fourier series

$$p(t) = \sum_{\ell=-\infty}^{\ell=\infty} P_{\ell} e^{j(\ell 2\pi/T)t} \quad (2.26)$$

In general the Fourier coefficients P_{ℓ} are given by

$$P_{\ell} = \frac{1}{T} \int_{t=0}^{t=T/N} p(t) e^{-j(\ell 2\pi/T)t} dt \quad (2.27)$$

where $p(t) = 1$ in the interval $t < T/N$.

Performing the operation indicated, it is seen that the coefficients are given by

$$P_{\ell} = \frac{e^{-j(\ell\pi/N)}}{N} \frac{\sin(\ell\pi/N)}{\ell\pi/N} \quad (2.28)$$

Assume that the input and output modulating functions $p(t)$ and $q(t)$ are identical; that is, $p(t) = q(t)$. Hence $P_{\ell} = Q_{\ell}$. Since both $p(t)$ and $q(t)$ are real, the Fourier coefficients P_{ℓ} and Q_{ℓ} must satisfy the relation

$$A_{-n} = A_n^* \quad (2.29)$$

Now (2.20) and (2.21) may be used to write a system function for the N -path network with binary modulators:

$$T(j\omega) = N \sum_{\ell=-\infty}^{\ell=\infty} P_{-\ell} P_{\ell} H(j\omega - j\ell\omega_0) \quad (2.30)$$

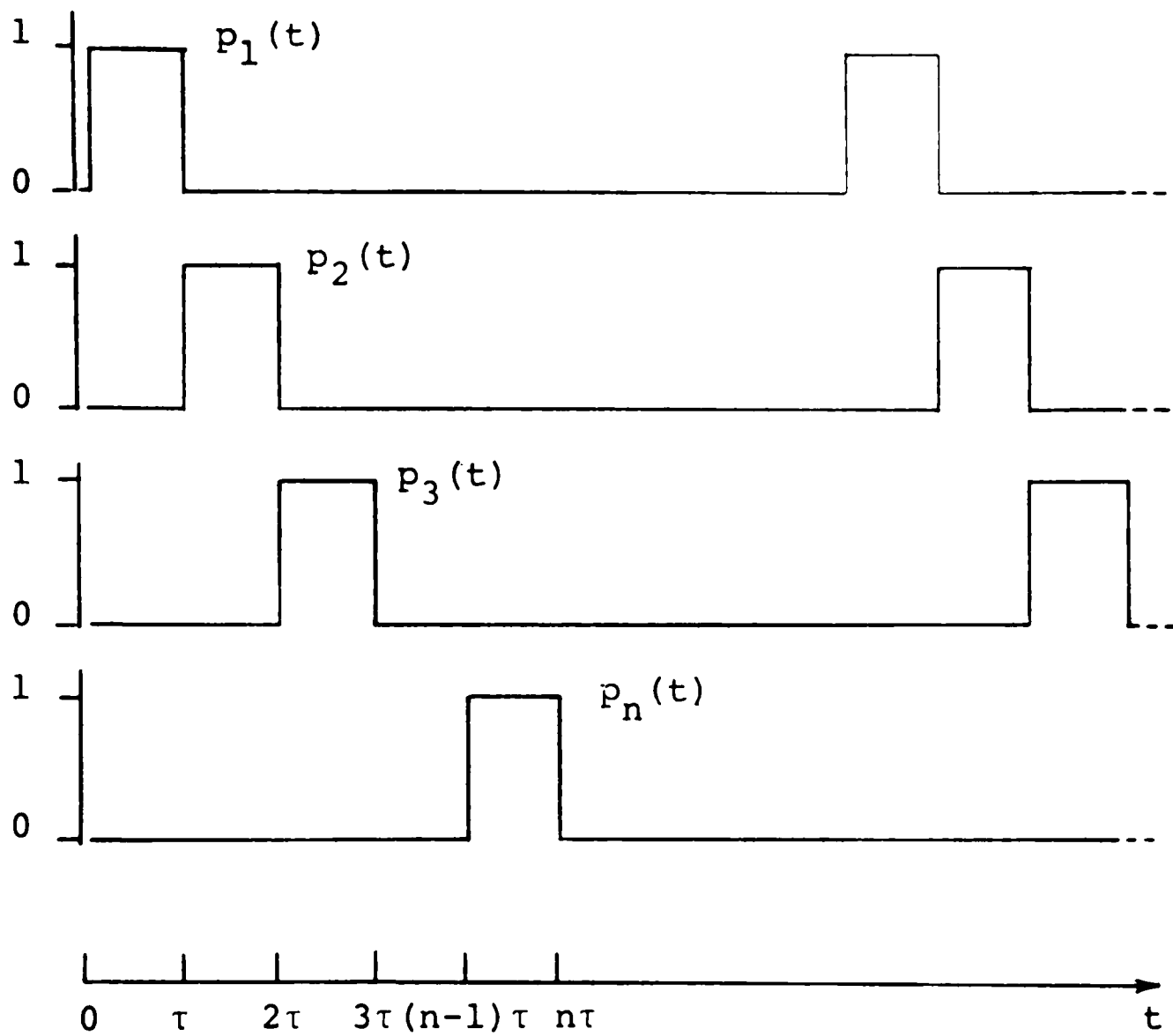


Figure 2.3. Modulating functions $p_n(t)$ produced by periodic switching.

Because of the band-limiting constraint on $T(j\omega)$, (2.30) can be approximated by the truncated series

$$T(j\omega) \approx \frac{1}{N} \sum_{\ell=-N/2}^{\ell=N/2} P_{\ell} P_{\ell}^* H(j\omega - j\ell\omega_0) . \quad (2.31)$$

It is understood that N must be even if the summation is to represent the network uniquely. Noting that

$$P_{\ell} P_{\ell}^* = |P_{\ell}|^2, \quad (2.31) \text{ becomes}$$

$$T(j\omega) \approx \frac{1}{N} \sum_{\ell=-N/2}^{\ell=N/2} \left[\frac{\sin(\ell\pi/N)}{\ell\pi/N} \right]^2 H(j\omega - j\ell\omega_0) . \quad (2.32)$$

For $N \geq 2$, $T(j\omega)$ has some interesting properties. If the cutoff frequency of the low-pass filters is small with respect to the signal frequency $\omega_0/2\pi$, the system function will have a sequence of narrow, equally spaced passbands of the same shape. The amplitudes are nearly equal, each centered about a multiple of ω_0 . Filters having this type of multiple passband response are usually denoted "comb filters", and are useful in recovering periodic waveforms from wide-band noise. A plot of $|T(j\omega)|$ versus ω is shown in Figure 2.4 for $N = 8$.

Returning to (2.32), it is evident that the terms inside the summation can be grouped in pairs having the general form

$$A_{\ell} [H(j\omega - j\ell\omega_0) + H(j\omega + j\ell\omega_0)] , \quad (2.33)$$

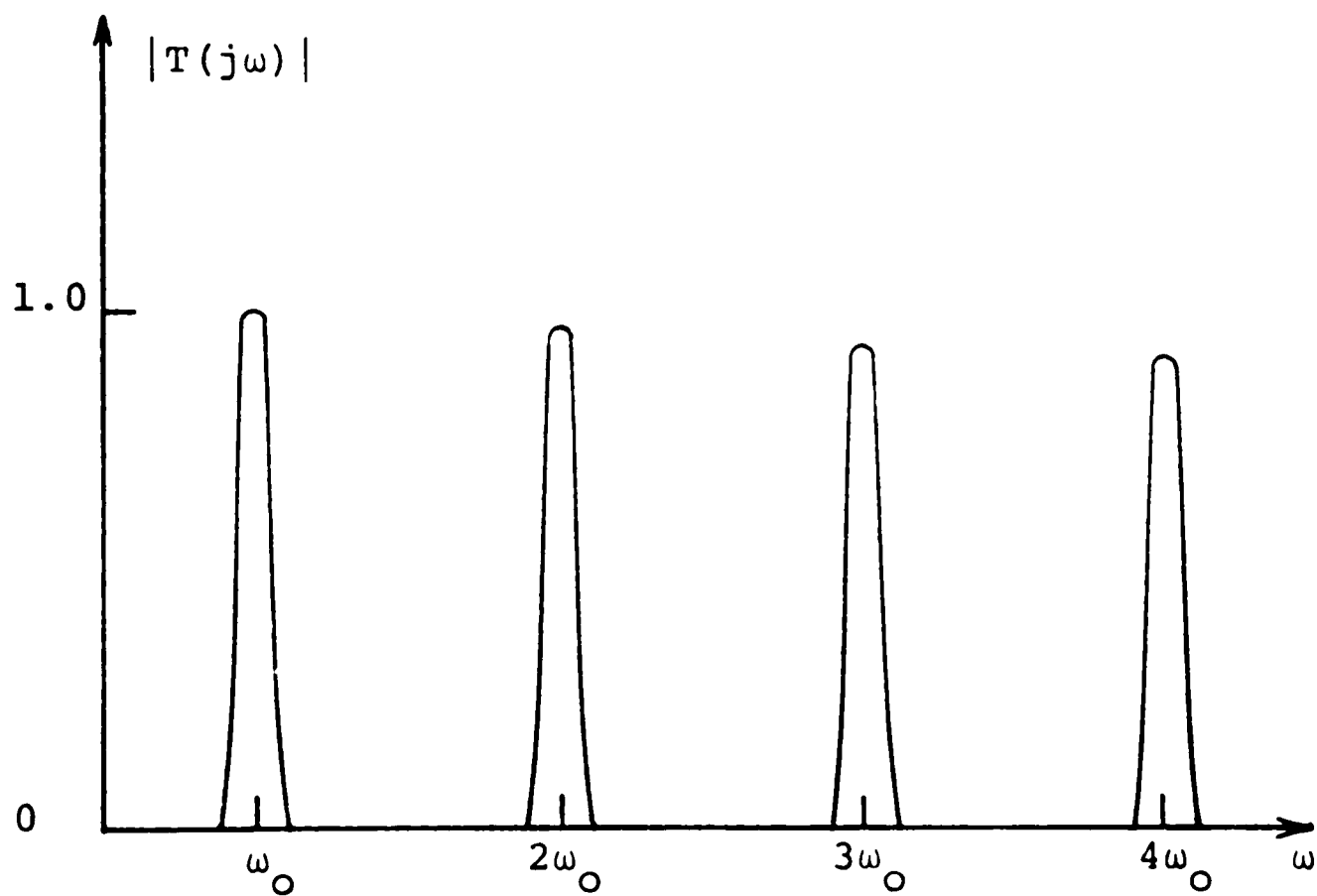


Figure 2.4. Plot of $|T(j\omega)|$ versus ω for N-path filter with $N=8$.

$$\text{where } A_\ell = \left[\frac{\sin(\ell\pi/N)}{\ell\pi/N} \right]^2 \quad . \quad (2.34)$$

The inverse Fourier transform of (2.32) can be expressed in general as

$$f(t) = F^{-1}[T(j\omega)] = \frac{2}{N} \sum_{\ell=-N/2}^{\ell=N/2} A_\ell h(t) \cos(\ell\omega_0 t), \quad (2.35)$$

where $h(t)$ is the impulse response of the low-pass filters in Fig. 2.1. Because of the time-varying modulating functions, $f(t)$ does not represent the impulse response of the N -path filter in the conventional sense. In general, the impulse response of a band-pass filter will have the form $f(t) = h(t) \cos(\omega_0 t)$. The term $h(t)$ has the form of a low-pass filter impulse response. This term determines the shape of the envelope of $|T(j\omega)|$, and therefore determines the bandwidth and Q -factor of the band-pass filter. The oscillatory part of the impulse response, the term $\cos(\omega_0 t)$, determines the center frequency. In conventional band-pass filters, the center frequency ω_0 is usually determined by the values of passive circuit elements. In the N -path filter, the oscillatory part of the impulse response is generated by multiplication of voltages in the filter by the modulating functions. The period T of the modulating functions can be controlled by means external to the N -path filter. Hence, if the modulating functions are phase or frequency-modulated,

the frequency of the oscillatory part of the impulse response (the cosine term in (2.35)) may be made time-varying. This modification of the oscillatory part of the impulse response of the N-path filter causes the filter to generate some particular band-pass characteristics distinct from those of conventional band-pass filter. An examination of the behavior of (2.35) for the case of frequency modulation is of interest.

A System Function for Frequency Modulated Signals

A time-varying term $\omega(t)$ may be substituted into (2.35) in place of ω_0 . The resulting equation then may be Fourier transformed to determine how a particular form of $\omega_0(t)$ affects the band-pass characteristics of the filter. The instantaneous frequency, which is now a function of time, can be written as

$$\omega(t) = \omega_0 + 2\pi A e_s(t), \quad (2.36)$$

where A is a constant and $e_s(t)$ is a modulating signal. It is convenient to specify a sinusoidal function for $e_s(t)$ to simplify later calculations. Let

$$e_s(t) = E_s \cos(\omega_s t + \theta), \quad (2.37)$$

where E_s and θ are constants and $\omega_s/2\pi$ is a modulating frequency. Substituting (2.37) into (2.36), it is seen

that

$$\begin{aligned}\omega(t) &= \omega_0 + 2\pi A E_s \cos(\omega_s t + \theta) \\ &= \omega_0 + 2\pi \Delta f \cos(\omega_s t + \theta),\end{aligned}\quad (2.38)$$

where $\Delta f = A E_s$ is called the "frequency deviation". The phase angle $\phi(t)$ is found by integrating $\omega(t)$ with respect to time:

$$\phi(t) = \int_0^t \omega(t) dt = \omega_0 t + B \sin(\omega_s t + \theta) + \phi, \quad (2.39)$$

where ϕ is a constant of integration. The constant B is denoted the "modulation index", or "frequency deviation ratio". Substituting $\phi(t)$ for $\omega_0(t)$ in the argument of the cosine term in (2.35) yields the equation

$$\begin{aligned}F^{-1}[T(j\omega)] &\approx \frac{2}{N} \sum_{\ell=0}^{\ell=N/2} A_{\ell} h(t) \cos[\ell(\omega_0 t + B \sin(\omega_s t + \theta) + \phi)] \\ &\approx \frac{2}{N} \sum_{\ell=0}^{\ell=N/2} A_{\ell} h(t) \{ \cos \ell(\omega_0 t + \phi) \cos[\ell B \sin(\omega_s t + \theta)] \\ &\quad - \sin \ell(\omega_0 t + \phi) \sin[\ell B \sin(\omega_s t + \theta)] \},\end{aligned}\quad (2.40)$$

where ℓB is the modified modulation index. The following Bessel function relationships will be used to expand the sinusoids containing sinusoidal arguments:

$$\cos[\ell B \sin(\omega_s t + \theta)] = J_0(\ell B) + 2 \sum_{n=1}^{n=\infty} J_{2n}(\ell B) \cos 2n(\omega_s t + \theta) \quad (2.41)$$

$$\sin[\ell B \sin(\omega_s t + \theta)] = 2 \sum_{n=0}^{\infty} J_{2n+1}(\ell B) \sin(2n+1)(\omega_s t + \theta) \quad (2.42)$$

These Bessel functions of the first kind, order m , are given by the series

$$J_m(\ell B) = \sum_{k=0}^{\infty} \frac{(-1)^k (\ell B/2)^{2k+m}}{k! (k+m)!} \quad (2.43)$$

Equation (2.40) can be written as

$$\begin{aligned} F^{-1}[T(j\omega)] \approx & \frac{2}{N} \sum_{\ell=0}^{\ell=n/2} A_{\ell} h(t) \{ \cos \ell(\omega_0 t + \phi) [J_0(B) \\ & + 2 \sum_{n=1}^{\infty} J_{2n}(\ell B) \cos 2n(\omega_s t + \theta)] \\ & - \sin \ell(\omega_0 t + \phi) [2 \sum_{n=0}^{\infty} J_{2n+1}(\ell B) \sin(2n+1)(\omega_s t + \theta)] \}. \quad (2.44) \end{aligned}$$

If the Fourier transform of (2.44) is taken, the system function of the N -path filter operating with input and output modulating functions, which are themselves frequency modulated, will be found. If the modified modulation index is small enough so that $\ell B \ll 1$, certain simplifying approximations may be made. Referring to (2.43), all Bessel functions $J_n(\ell B)$ are negligible except for $n = 0, 1$. Furthermore,

$$J_0(\ell B) \approx 1, \quad \ell B \ll 1 \quad (2.45)$$

and

$$J_1(\ell B) \approx \ell B/2, \quad \ell B \ll 1. \quad (2.46)$$

Substituting (2.45) and (2.46) into (2.44) results in

$$\begin{aligned} F^{-1}[T(j\omega)] \approx & \frac{2}{N} \sum_{\ell=0}^{\ell=N/2} A_{\ell} h(t) \{ \cos \ell(\omega_0 t + \phi) \\ & + \frac{\ell B}{2} \cos[(\ell\omega_0 + \omega_s)t + \ell\phi + \theta] \\ & - \frac{\ell B}{2} \cos[(\ell\omega_0 - \omega_s)t + \ell\phi - \theta] \}. \end{aligned} \quad (2.47)$$

The Fourier transform of (2.47) may be taken to determine the system function $T(j\omega)$. It is of interest to calculate the magnitude of the system function, $|T(j\omega)|$, as a function of ω . Taking the Fourier transform of (2.47), and dropping the phase terms containing ϕ and θ which do not affect the magnitude, yields

$$\begin{aligned} |T(j\omega)| \approx & \frac{1}{N} \sum_{\ell=-N/2}^{\ell=N/2} A_{\ell} |H(j\omega - j\ell\omega_0) + \frac{\ell B}{2} H(j\omega - j\ell\omega_0 - j\omega_s) \\ & - \frac{\ell B}{2} H(j\omega - j\ell\omega_0 + j\omega_s)|. \end{aligned} \quad (2.48)$$

This system function has, for each value of ℓ , three band-pass "windows". One is centered about $\ell\omega_0/2\pi$, the other two are separated from $\ell\omega_0/2\pi$ by $\pm\omega_s/2\pi$. This is in direct analogy to the frequency spectrum of a

narrow-band, frequency-modulated wave of carrier frequency $\omega_c/2\pi$, modulated by a sinusoidal signal of frequency $\omega_s/2\pi$. Evidently, the system function of the N-path filter operating in the frequency-modulated mode is matched to the spectral components of a frequency-modulated signal with carrier frequency $\omega_c/2\pi$, modulating frequency $\omega_s/2\pi$, and modulation index B. It is shown in Appendix A that the system function given by (2.40) can, in general, match the frequency components of a periodic, non-sinusoidal, band-limited signal which may be frequency-modulated.

Noise Bandwidth of the N-path Filter

The matched-filter system function which may be generated by the N-path filter may be useful in increasing the signal/noise ratio of a frequency-modulated waveform. Specifically, the filter may be made to exhibit a noise bandwidth less than the bandwidth occupied by all of the components of the spectrum of the signal being filtered.

A traditional method of estimating the bandwidth required for reception of a frequency-modulated signal is based upon the observation that $J_n(\ell B)$, as a function of n , decreases rapidly for $n > \ell B$. If only the first $n \leq \ell B$ Bessel functions are considered significant, the highest modulating frequency of interest is then $\omega_{sm} \ell B/2\pi$, where $\omega_{sm}/\ell B$ is the maximum modulating frequency. Hence the approximate bandwidth, W , of an ideal filter

which will pass all significant components in the signal spectrum is given by

$$W \approx 2\omega_{sm} \text{ radians/sec} \quad . \quad (2.49)$$

The equivalent-noise bandwidth of a non-ideal filter is defined as the bandwidth of an ideal filter which has the same output noise power as the non-ideal filter, for a given Gaussian, white noise input.

For example, consider the N-path filter with single pole, R-C low-pass filters having the transfer function

$$H(s) = \frac{1/RC}{s + 1/RC} \quad . \quad (2.50)$$

The equivalent-noise bandwidth, W_{eq} , for the low-pass filter having the function given by (2.50) has been calculated and is

$$W_{eq} = 1/4RC \text{ radians/sec [3]} \quad . \quad (2.51)$$

If it is assumed that the filter modulating functions introduce no noise, the equivalent-noise bandwidth of the N-path filter for the narrow-band, frequency-modulated case may be calculated using (2.48) and (2.51). Equation (2.51) may be substituted into (2.48) in place of the

three terms $H(j\omega - j\ell\omega_0)$, $H(j\omega - j\ell\omega_0 - j\omega_s)$, and $H(j\omega - j\omega_0 + j\omega_s)$. Performing the summation indicated in (2.48) yields the total equivalent-noise bandwidth W_t of the N-path filter, giving

$$\begin{aligned} W_t &= \frac{1}{N} \sum_{\ell=-N/2}^{\ell=N/2} A_\ell W_{eq}[1 + \ell B] \\ &= \frac{1}{4NRC} \sum_{\ell=-N/2}^{\ell=N/2} A_\ell [1 + \ell B], \quad \ell B \ll 1. \end{aligned} \quad (2.52)$$

An equivalent-noise bandwidth improvement factor F_n may be defined, using (2.52) and (2.49), as

$$F_n = \frac{W}{W_t} = 8NRC\omega_{sm} \sum_{\ell=-N/2}^{\ell=N/2} A_\ell [1 + \ell B]^{-1}, \quad \ell B \ll 1. \quad (2.53)$$

Equation (2.53) may be considered to be a noise bandwidth improvement factor over classical techniques for wide-band, white noise. The term F_n gives the ratio of the output noise power of a rectangular band-pass filter with bandwidth sufficient to pass all significant frequency components of the frequency-modulated signal, to the output noise power of the N-path filter. Because the term W_t may be made arbitrarily small by increasing N , R and C , the quantity F_n may be made quite large. If $F_n \gg 1$, the N-path filter has an equivalent-noise bandwidth which is less than the effective signal

bandwidth. This result indicates that, at least in principle, signals with arbitrarily low signal/noise power ratios may be enhanced by the N-path filter.

Obtaining Modulating Functions for the N-path Filter

Very precise synchronization of the filter modulating functions and the filter input signals is necessary for the stable operation of the N-path filter at very narrow bandwidths. Also, the modulating functions must track the input signal if a matched-filter system function is to be generated. A phase-locked loop and digital circuitry may be used to derive modulating functions from a reference signal which may be frequency or phase-modulated. The reference signal may be a noisy signal which is applied to the N-path filter, the signal which appears at the output of the N-path filter, or some external signal. If the reference signal is derived from the input or output of the N-path filter, the modulating functions may be forced to vary in frequency in a manner which causes the N-path filter to track the signal being filtered. In this case, the N-path filter is adaptive and may generate a matched system function from swept-frequency or frequency-modulated signals.

Because of the importance of the phase-locked loop in the adaptive N-path filter, a discussion of a general phase-locked loop has been included in Appendix B.

It is necessary to derive from the reference signal a series of N periodic pulse trains having pulse width $\tau = T/N$ and period T . These N pulse trains correspond to the N binary modulating functions $p[t]$, $p[t - \tau]$, ..., $p[t - (N-1)\tau]$ (see Fig. 2.3). Ideally the reference signal and the sampling pulses should be "phase coherent", that is, the k th sampling pulse should start at the same point in phase ϕ_k of the reference signal on each successive cycle.

In the system to be described, a phase-locked loop having a programmable frequency divider inserted between the VCO output and the phase detector input is used as a coherent frequency multiplier. As shown in Fig. 2.5, the input signal frequency is $f_i = 1/T$ hertz. The reference signal, which is phase-locked to the input signal, appears at the output of the divide-by- $N/2$ counter. The frequency of the reference signal is f_i hertz when the loop is phase-locked; thus the frequency of the square wave signal at the input of the divide-by- $N/2$ counter is $f_o = \frac{N}{2}f_i$ hertz. The coherent reference signal of frequency $\frac{N}{2}f_i$ may be applied to a binary counter which counts low-high and high-low level transitions of the signal. The output of the counter is a binary number which may have the values $0, 1, 2, \dots, (N-1), 0, 1, 2, \dots$. A decoding circuit with N outputs converts the binary output of the counter to a series of sequential pulses having width T/N , and period T , which are

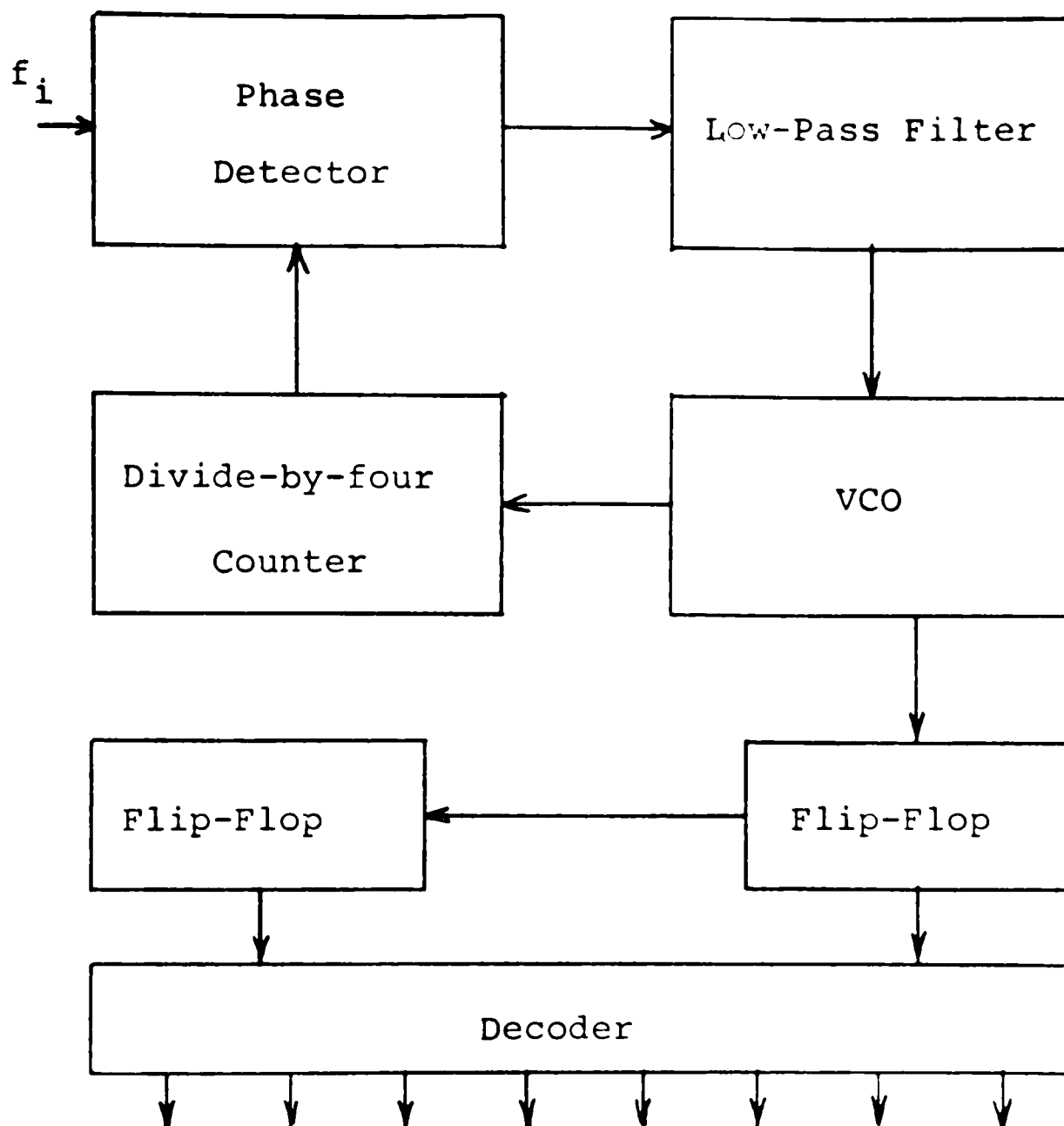


Figure 2.5. Block diagram of elementary phase-locked loop and decoding network.

phase-coherent with the input signal to the phase-locked loop. These sampling pulses control switching transistors in the N-path network which simulate analog multipliers having binary modulating functions.

CHAPTER III

DESIGN AND EXPERIMENTAL DEMONSTRATION OF AN ADAPTIVE N-PATH FILTER

The mechanization of an adaptive N-path filter with modulating functions generated by a phase-locked loop is the subject of this chapter. The development of a circuit requires the design of three major functional groups:

- 1) an N-path filter and switching modulators,
- 2) a phase-locked loop with a divide-by-four counter in the feedback loop,
- 3) a three-bit counter and decoding logic with field effect transistor gate drivers.

A block diagram of the system is shown in Figure 3.1. It is necessary to interface each functional group with the others through level translating circuits or buffer amplifiers.

Design of the N-path Filter

To simplify the design of the digital logic circuits, the filter is constructed using eight sections, that is $N = 8$. The capacitors which form the low-pass filters are chosen to give a 0.25 second time constant with a resistance of approximately $1\text{ M } \Omega$. This time constant corresponds to a filter -3 dB bandwidth of 1 hertz. The input to the filter is through potentiometer R_1 . Setting R_1 controls the effective Q and bandwidth of the N-path filter. Capacitors used in the filter are $0.24\text{ } \mu\text{F}$ units matched to within $\pm 0.18\%$. Field effect transistors (FET's) are used for

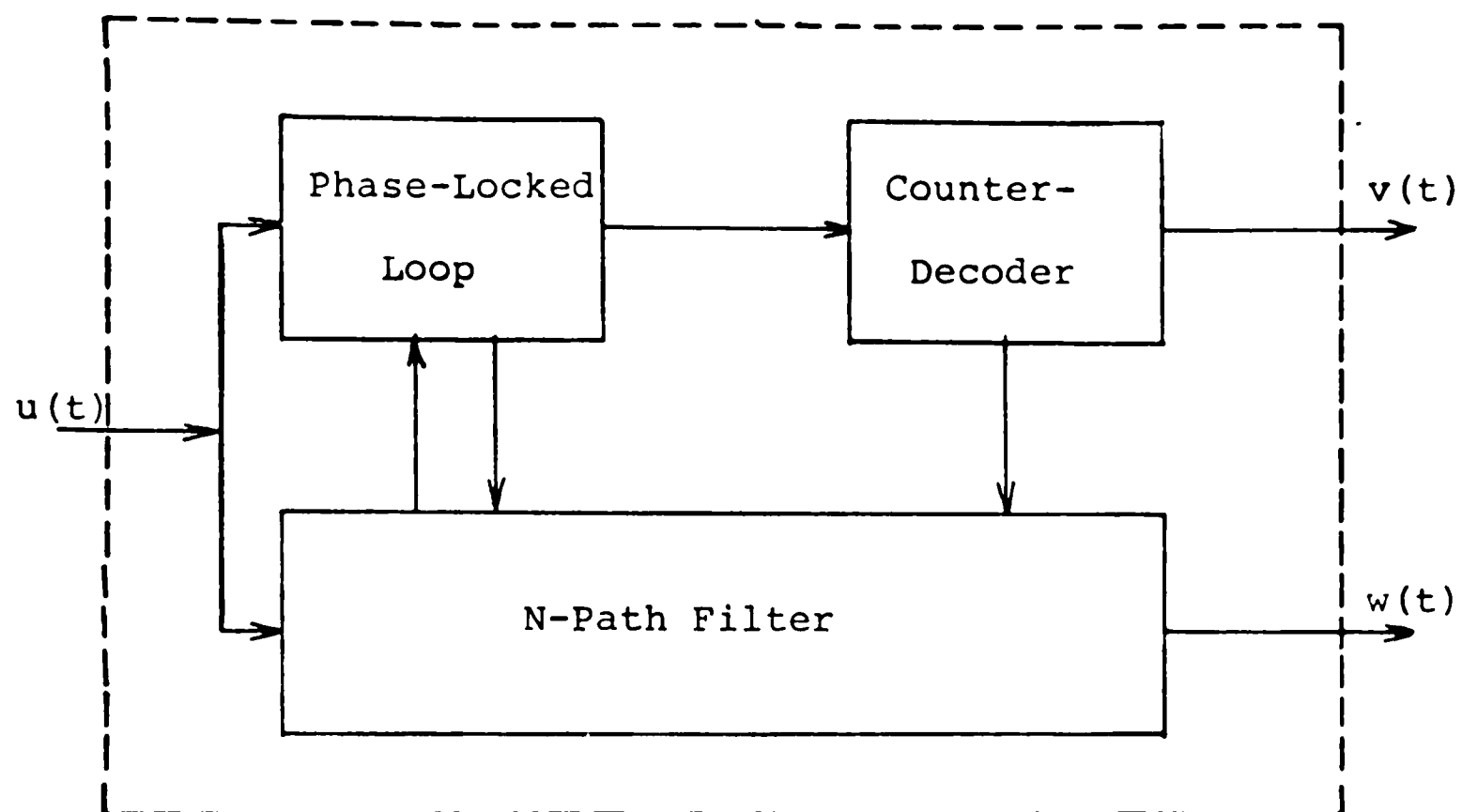


Figure 3.1. Block diagram of the adaptive N-path filter.

the switching modulators. FET's may be operated as voltage controlled resistors with very low saturation voltage, and typically have a ratio of off resistance to on resistance of greater than 10^5 . The low FET gate-drain capacitance ($< 5\text{pF}$) limits feed through of the gate control pulses, thereby limiting switching noise. A high input impedance, common-drain amplifier stage was added to the N-path filter output to reduce loading of the filter by the phase-locked loop. The very high input resistance of the common-drain stage allows the insertion loss of the N-path filter to be made negligibly small, even for very narrow bandwidths and large values of the filter input resistor R_1 . A diagram of the eight section filter is shown in Fig. 3.2. Two D-type flip-flops connected in cascade form the divide-by-four counter which is inserted between the VCO output and the phase detector of the phase-locked loop. A common collector amplifier between the VCO output and the clock signal input of the first flip-flop provides dc level translation to match the level of the VCO output by the digital circuitry.

An integrated phase-locked loop, with transistor-transistor logic (TTL) compatible VCO output and phase detector inputs, is used. This phase-locked loop is designed to be used with an external R-C filter to simulate type 2 operation (see Appendix B). The component values

of this R-C filter are chosen from curves supplied by the manufacturer of the phase-locked loop, to provide a loop damping ratio of 0.707. These curves are adjusted to compensate for the reduction in loop gain caused by the insertion of the divide-by-four counter in the loop. With a VCO free-running frequency of 20 kHz, corresponding to a fundamental frequency of 5.0 kHz, the VCO control voltage has a 15% overshoot in response to a step frequency change of 500 Hz at the phase-locked loop input. The loop remained phase-locked over a frequency range of 1.2 kHz to 8.8 kHz.

The input of the phase-locked loop may be connected by means of a switch S to the N-path filter input, output, or to an external source. If the loop input is taken from the filter input or output, the loop can synchronize to and track the signal which is being filtered. In this mode, the fundamental frequency component of the signal is recovered through the narrow-band filtering action of the phase-locked loop, and it is used to generate the filter sampling pulses. When the loop is synchronized to a noise-reference signal through the external input, the N-path filter acts as a conventional signal sampler. The adaptive nature of the system is retained in this mode also, allowing the sampling of frequency-swept, phase or frequency-modulated signals.

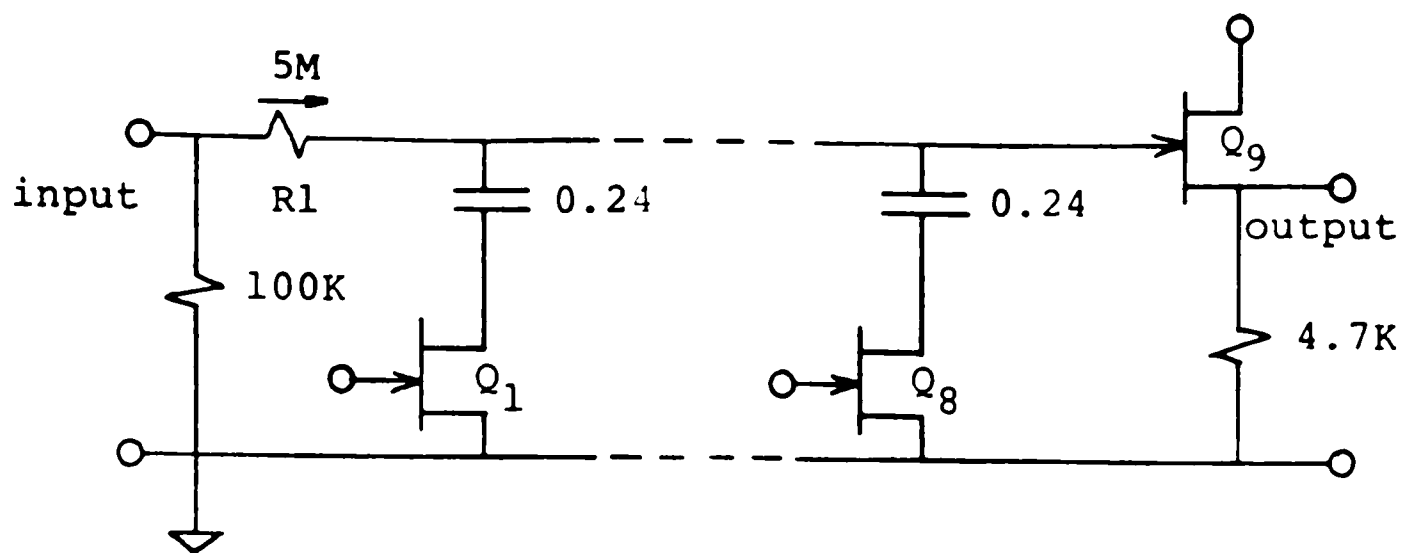


Figure 3.2. Diagram of the eight-path filter.

The Phase-locked Loop and Decoding Network

The phase-locked loop and decoding network are shown in Figure 3.3.

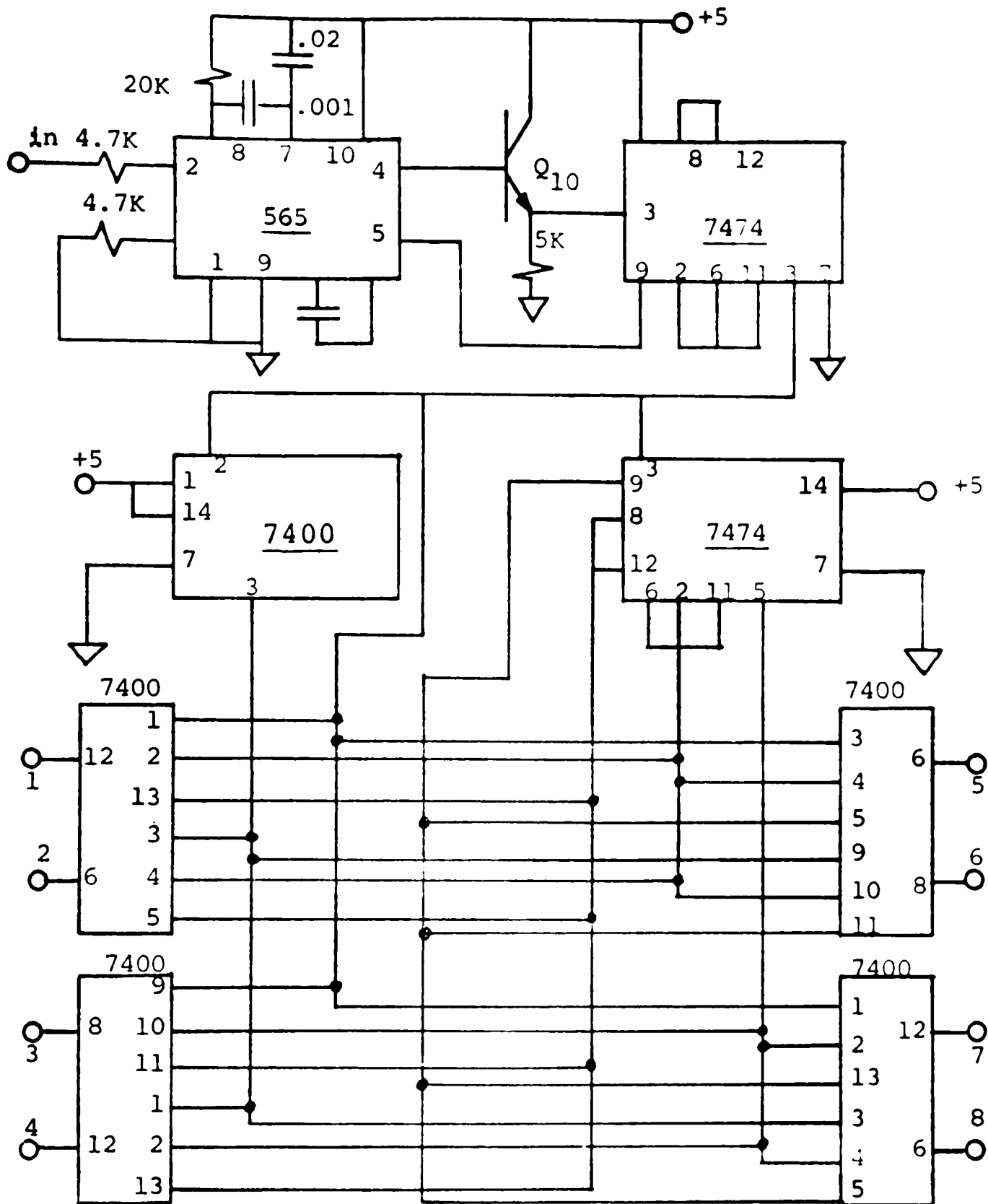


Figure 3.3. Phase-locked loop and decoding network.

The decoding network which is shown in Fig. 3.3 consists of nine, three-input TTL nand gates. One gate is used to complement the VCO output signal. The outputs of the other eight nand gates serve as inputs to the FET gate drivers, transistors $Q_1 - Q_8$. The decoder gates have high levels of 3.5 V, and low levels of 0.4 V. It is necessary to drive the FET gates to a level of 0.0 V, corresponding to an "on" state, and to a level of -10 V, corresponding to an "off" state. The FET "on" state must occur when a decoder gate output is in the low state. The FET-compatible gate drivers perform the required inversion and level translation of the nand gate outputs.

The choice of suitable FET's for the filter depends upon the expected signal levels and the operating frequency. In general, FET's having a high conductance at saturation are suitable for low level signals, but FET's of this type usually have large gate areas and poor high-frequency performance. High-frequency FET's generally have lower conductance at saturation, and are not as desirable for low Q-factor filters or low level signals. The FET's used in the demonstration N-path filter are a low-noise, high-conductance, low-frequency type. While the phase-locked loop and logic components are capable of operation up to about 15 MHz, the FET's used in the design limit the upper operating frequency of the filter to about 100 kHz. The residual noise at the filter output with no applied signal

was very low, less than 1mV p-p.

Signal Sources Used in the Filter Evaluation

The signal sources used in the filter measurements are shown in Fig. 3.4. The function generator F_1 provides signals which can frequency-modulate the sine wave output of the coherent decade frequency synthesizer. The function generator F_1 can also frequency-modulate a second function generator F_2 . Function generator F_2 can provide frequency-modulated sine, triangular, ramp, square, and pulse waveforms.

The wide-band operational amplifier, A, is used to combine a signal from the synthesizer or function generator with wide-band noise from the noise source. The noise source, a Solitron Device type 500 MWN 29R 6750, is a solid state, hybrid device. The output noise spectrum was examined with a wavemeter and found to be essentially flat over the frequency range of 20 Hz - 100 kHz. Potentiometers R_2 , R_3 , and R_4 are used to set the signal/noise ratio and the level of the output signal plus noise.

Experimental Measurements

Some band-pass characteristics of the N-path filter which have been previously derived are verified by data presented in the following sections. In the next section the magnitude-frequency characteristics of the system

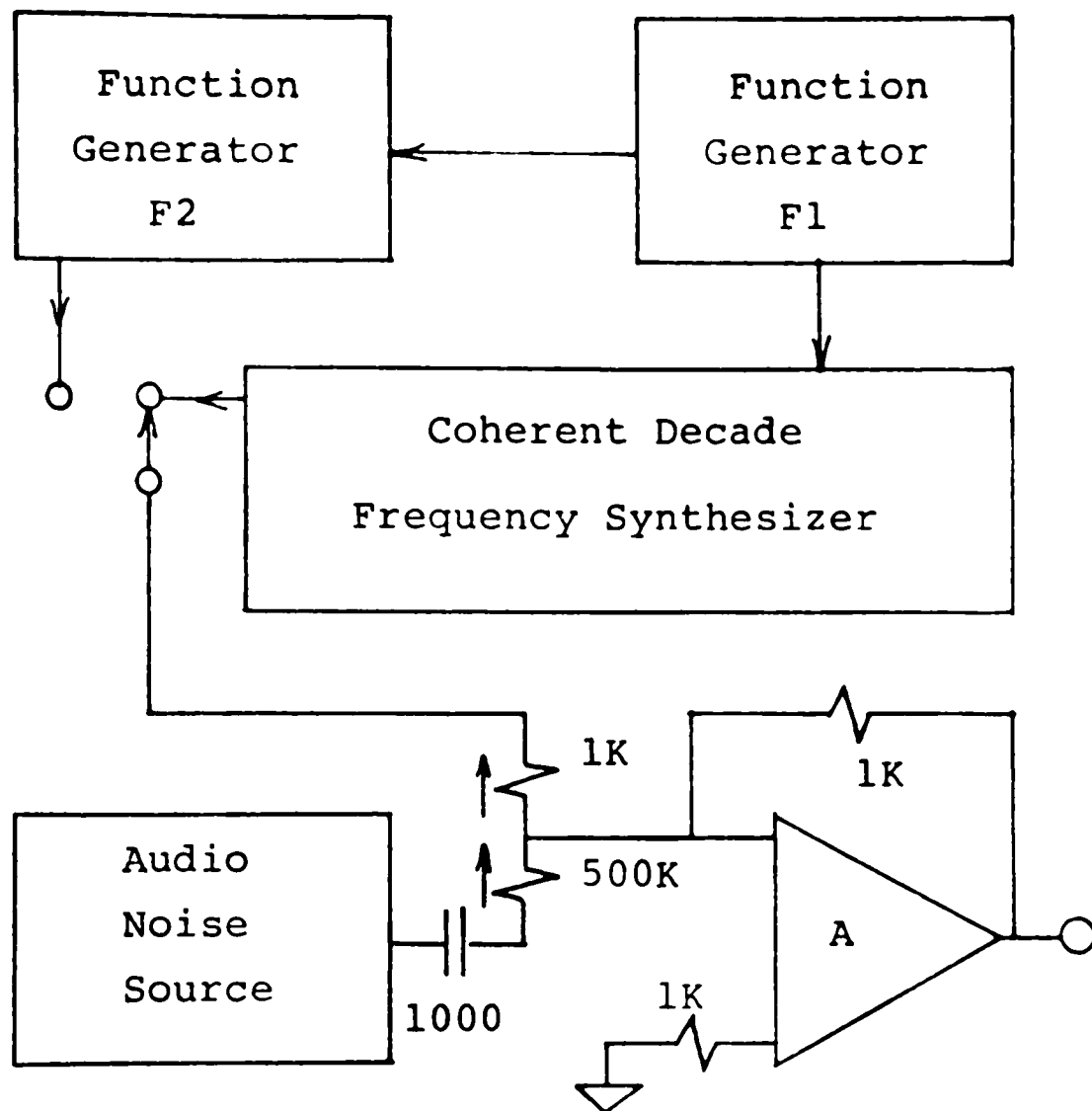


Figure 3.4. Signal sources used in the N-path filter measurements.

functions, given approximately by (2.32) and (2.48), are verified for noise-free, sinusoidal inputs to the N-path filter. Both constant-frequency and frequency-modulated operating modes of the filter are examined.

Photographs of oscilloscope traces showing sinusoidal and triangular waveforms filtered by the N-path filter are given in Figure 3.8 - 3.11.

A following section presents the results of adaptive filtering of noisy signals. Sinusoidal and non-sinusoidal, band-limited signals are filtered. The filter modulating functions are derived from the noise-free signal.

The last section considers the adaptive filtering of noisy sinusoidal signals which are narrow-band, frequency modulated. For this case, the input to the phase-locked loop is taken from the N-path filter output. The filter and phase-locked loop combination may act as a low threshold signal demodulator when operating in this mode.

Magnitude-frequency Characteristics of the N-path Filter, Sinusoidal Inputs

Figure 3.5 shows the measured band-pass, and the calculated band-pass for the N-path filter based on (2.32). The input to the filter was a 0.2 V RMS sine wave from the coherent decade frequency synthesizer. The phase-locked loop was driven by an unmodulated 5.0 kHz external reference signal. The input frequency was incremented in steps

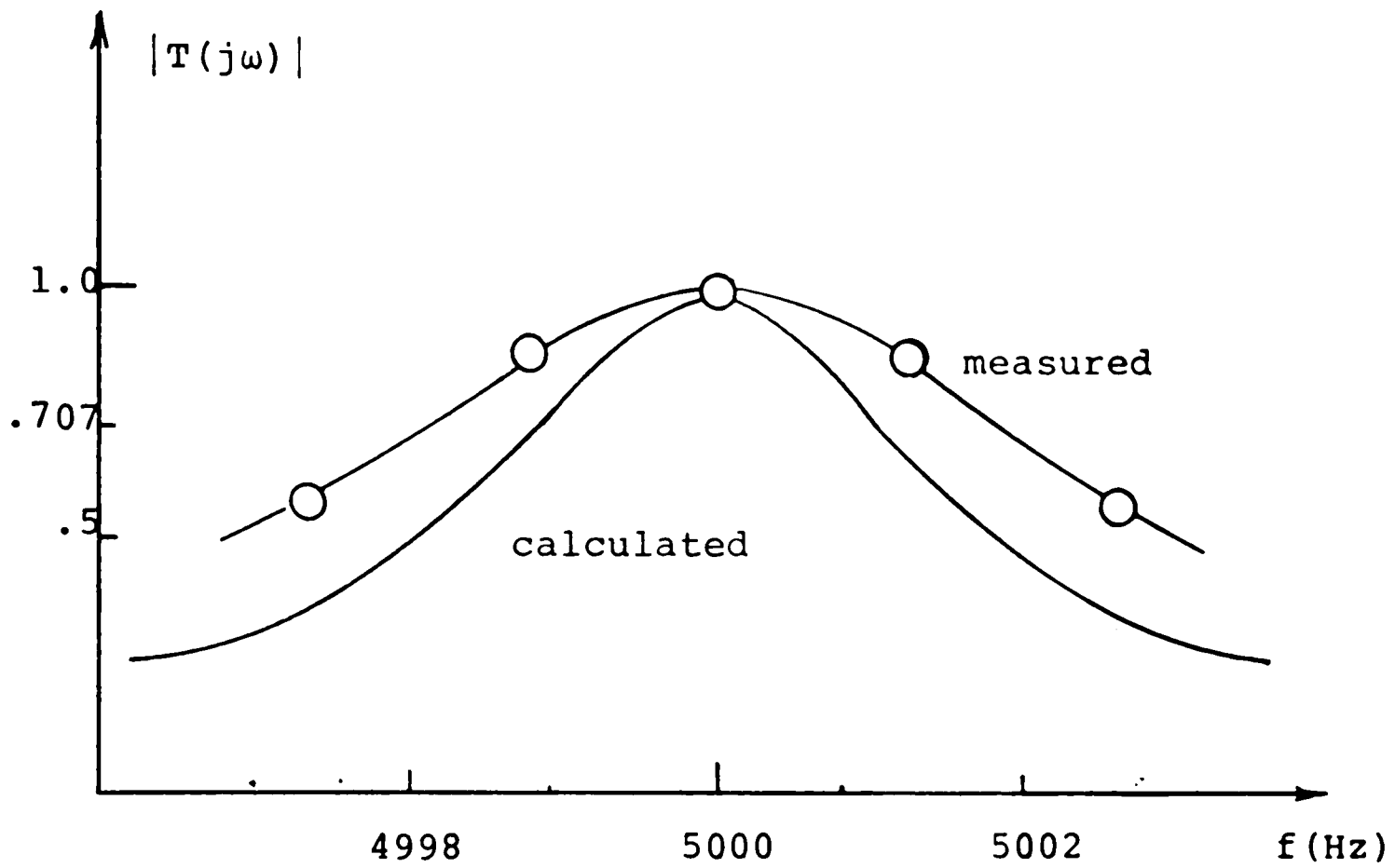


Figure 3.5. Magnitude-frequency plot of N-path filter system function, unmodulated case.

of 0.5 Hz to delineate the band-pass curve. Figure 3.6 clearly shows the "comb filter" response indicated by (2.32). The measured bandwidth of the curve in Figure 3.5 exceeds the calculated bandwidth; this effect is probably due to dispersion of the 5 kHz spectral line from the frequency synthesizer.

Figure 3.7 shows the band-pass characteristics for a sine wave input and frequency-modulated filter modulating function. The modulating functions have carrier frequency $f_c = 5$ kHz, modulating frequency $f_s = 50$ Hz, and modulation index $\ell B = 1$. The calculated band-pass curve is based on the approximate system function for the frequency-modulated case given by (2.48). The small spread between calculated and measured values evident in Figure 3.7 is the result of the modulation index not fulfilling the inequality $\ell B \ll 1$.

Adaptive Filtering of Noisy Signals, Externally Supplied Reference Frequency

Figures 3.8, 3.9, 3.10, and 3.11 show respectively sinusoidal, triangular, square, and pulse waveforms filtered from additive, wide-band noise. The filter modulating functions were derived from a noise-free replica of the signal in each case. In each photograph, the frequency of the signal is 5 kHz, the signal amplitude is 10 mV p-p,

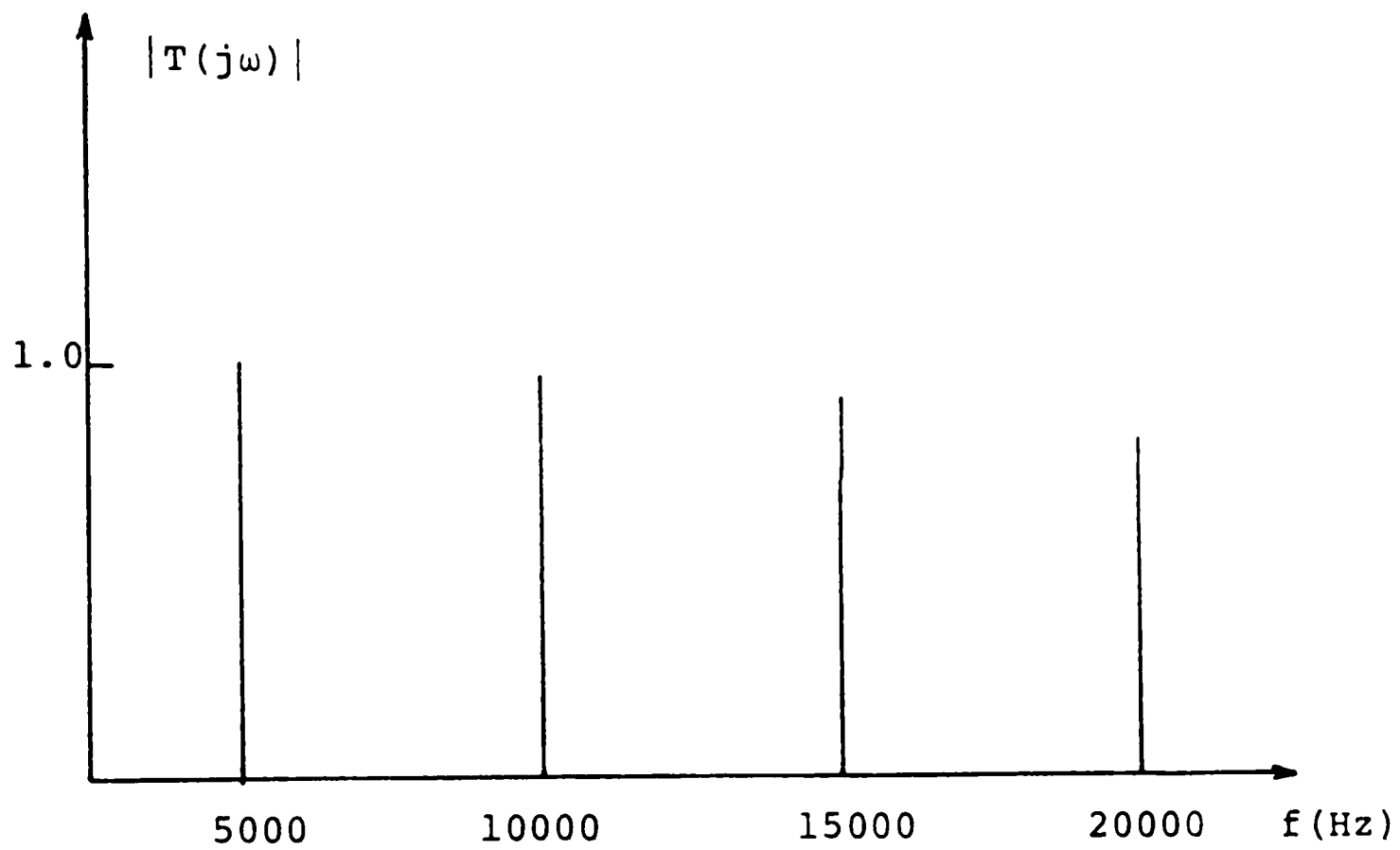


Figure 3.6. Magnitude-frequency plot showing "comb filter" response.

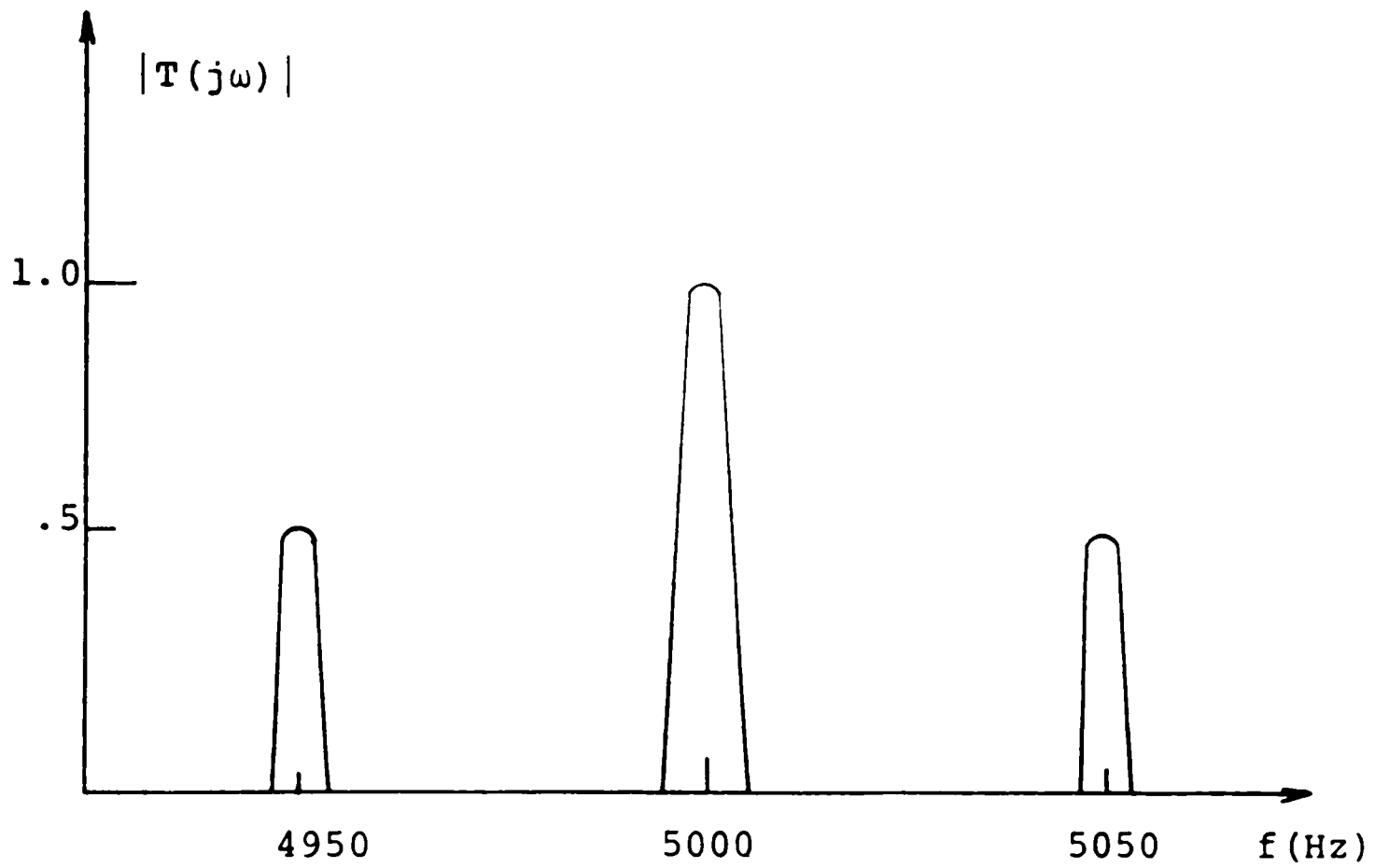


Figure 3.7. Magnitude-frequency plot of N-path filter system function, frequency-modulated case.

and the noise RMS amplitude is 2.5 V. The corresponding signal/noise ratio for the sine wave is -57 dB. Because the N-path filter can pass only $N/2 = 4$ harmonics, the waveforms in Fig. 3.9 - 3.11 become progressively more distorted, as the waves contain more energy at higher harmonics. Nevertheless, the noise content of the output signal, (the lower trace in each photograph) is visibly imperceptible in the time exposures presented. Estimating the output noise voltage conservatively as 2% of the signal voltage gives a signal/noise ratio of about 26 dB. The input-to-output signal/noise improvement ratio is then approximately 80 dB for the sine wave. Frequency-modulated inputs analogous to the signals in Fig. 3.8 - 3.11 give similar results. Noise performance of the filter in the frequency-modulated case is not visually distinguishable from the unmodulated case. The maximum modulating frequency for the system is 200 Hz, limited by the bandwidth of the type 2 phase-locked loop. The frequency deviation of the frequency-modulated signal is 50 Hz in each case.

Adaptive Filtering of Noisy, Frequency-Modulated Signals,
Reference Derived from the Filter Output

When the N-path filter modulating functions are derived from the output of the filter by means of the phase-locked loop, the filter and phase-locked loop system can operate

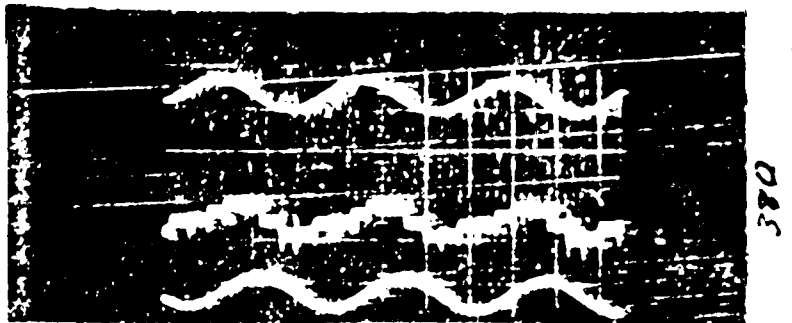


Figure 3.8. Sine wave filtered from wide-band noise.
Signal amplitude 10 mV p-p, noise 2.5V RMS.

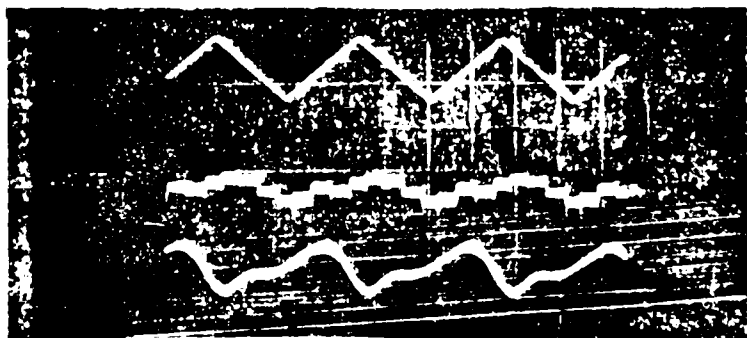


Figure 3.9. Triangular wave filtered from wide-band noise.
Signal amplitude 10 mV p-p, noise 2.5V RMS.



Figure 3.10. Square wave filtered from wide-band noise.
Signal amplitude 10 mV p-p, noise 2.5V RMS.

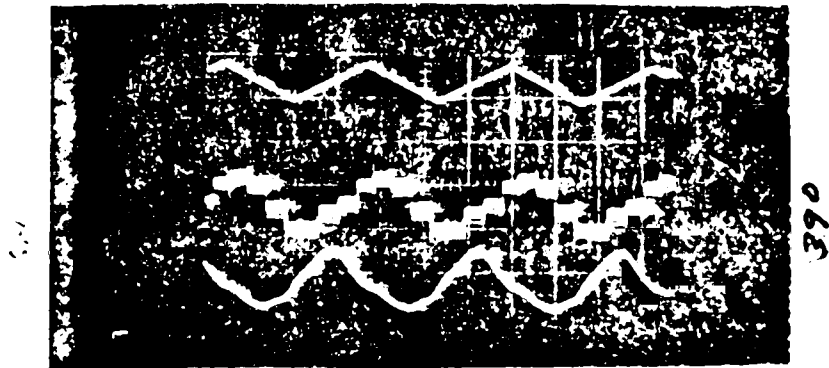


Figure 3.11. Pulses filtered from wide-band noise.
Signal amplitude 10 mV p-p, noise
2.5 V RMS.

without an external reference frequency. The system is capable of acting as an adaptive comb filter or a coherent demodulator for phase or frequency-modulated signals at low signal/noise ratios. Figure 3.12 shows a noisy, frequency-modulated sine wave filtered by the system. The input signal has amplitude 0.2 V p-p, carrier frequency $f_c = 5$ kHz, modulation frequency $f_s = 50$ Hz, and frequency deviation $f = 50$ Hz. Note in Fig. 3.12 that the frequency deviation of the filter output (lower trace) is less than that of the input (upper trace). This occurs because the filter system function has a magnitude less than unity at the upper and lower signal side-band frequencies. Hence the side-band components of the input signal are reduced in amplitude going through the filter. This corresponds to a reduction of the modulation index of the output signal. This is a property of the filter which may not be particularly detrimental. According to Van Cleave, most signals, especially speech and pulses, are quite recognizable if only the largest components of the signal spectrum are retained [4].

The maximum modulating frequency f_s for which the phase-locked loop will remain locked is strongly dependent upon the signal/noise ratio at the filter input and the amplitude of the input signal. Figure 3.13 is a plot of f_s max versus the input signal noise ratio for a signal level of 200 mV p-p. For signal/noise ratios greater than -25 dB,

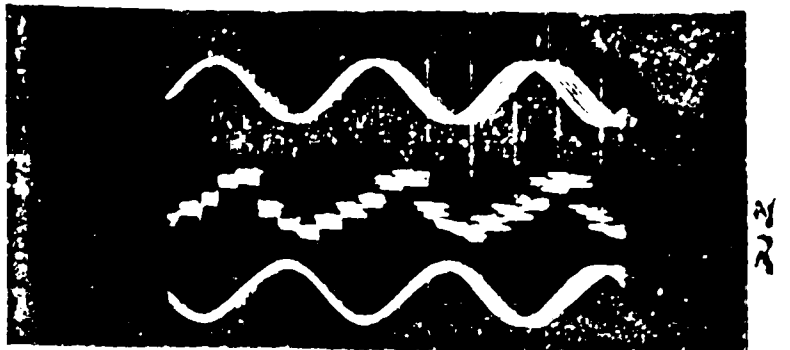


Figure 3.12. Frequency-modulated sine wave filtered from wide-band noise. Signal amplitude 200 m , noise amplitude 2.5 V RMS.

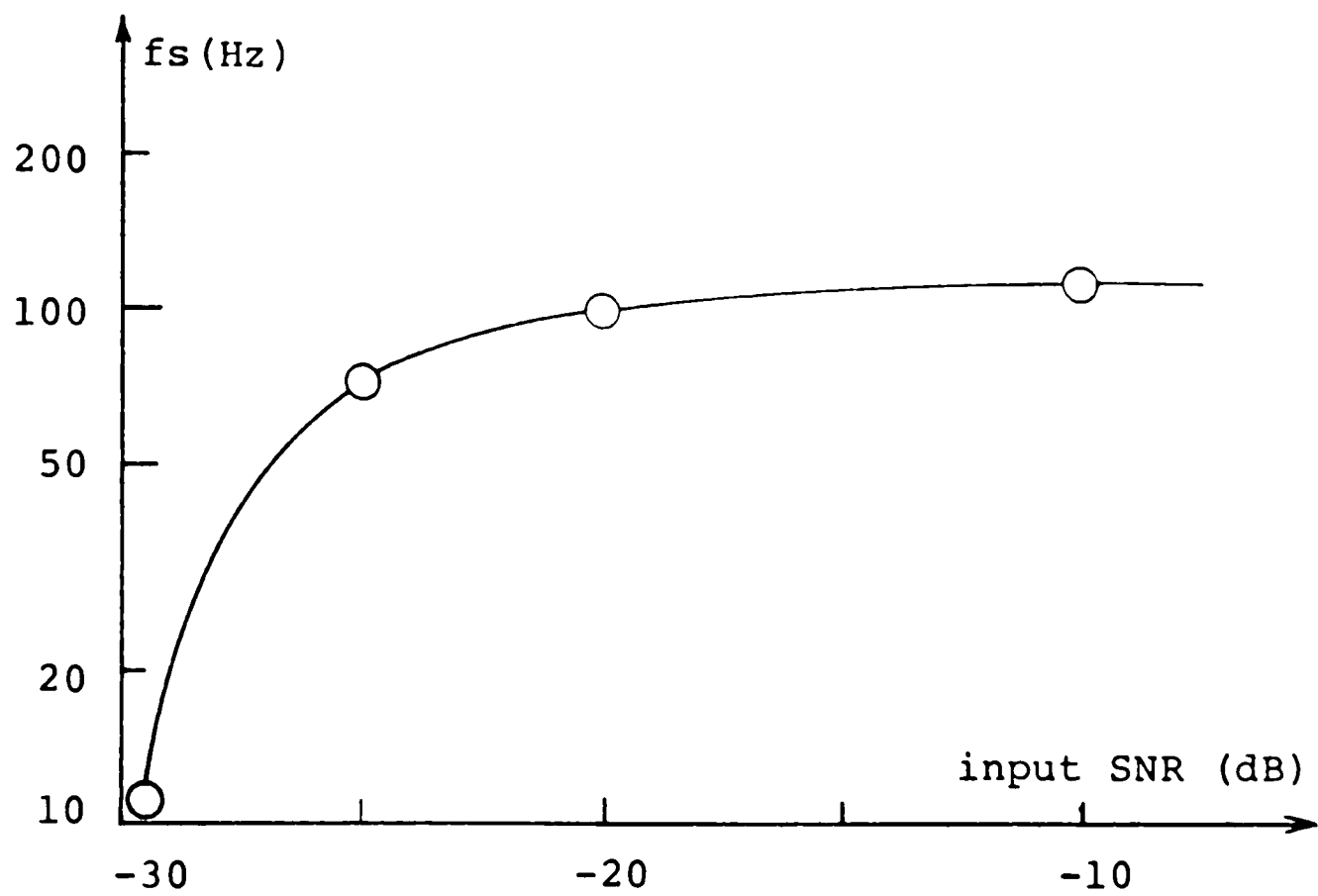


Figure 3.13. Maximum modulating frequency f_s as a function of input signal/noise ratio, signal amplitude 200 m p-p.

f_s max in Fig. 3.12 rapidly approaches a value which is nearly equal to the 200 Hz bandwidth of the type 2 phase-locked loop. With a -20 dB signal/noise ratio at the filter input, the loop remained phase-locked as the signal was swept from 1.2 kHz to 8.8 kHz, the lock range of the loop, at a sweep rate of 50 Hz/second. When the phase-locked loop was initially in a free-running condition, the system would reliably acquire the signals as it was swept past the loop free-running frequency at the 50 Hz/second rate. This result indicates that the N-path filter may be useful as a signal-acquisition system at low signal/noise ratios.

A limitation of the experimental system prevents the operation of the adaptive filter at signal/noise ratios less than about -30 dB. The phase-locked loop requires a signal amplitude of at least 200 mV p-p in order to achieve lock reliably, so the signal/noise ratio cannot be decreased by reducing the input. The N-path filter does not operate well if the input noise has peaks above 10 V, corresponding roughly to an RMS amplitude of 2.5 V. If the noise peaks exceed 10 V, the FET gates can become forward-biased during switching. This may cause several FET's to conduct simultaneously. As a result, very low signal/noise ratios, less than about -30 dB, could not be examined. It is likely that signal/noise ratios less than -30 dB could be investigated with a circuit optimized for very low signal/noise operation.

CHAPTER IV

CONCLUSIONS

The adaptive N-path filter is capable of generating a type of simple, very high Q, matched filter for periodic functions which are band-limited, phase or frequency-modulated or subject to frequency drift. The N-path filter may provide an equivalent-noise bandwidth for frequency-modulated signals which is less than that based on classical techniques. In principle, signals having arbitrarily low signal/noise ratios may be enhanced by the filter.

A number of approximations were made in the derivations of the system function for the N-path filter in Chapter II. The favorable agreement between the calculated and measured transfer characteristics, as shown in Figure 3.5-3.7, indicates that these approximations are valid for the cases which were considered. The behavior of the filter for the case of large modulation indices has not been investigated in detail. Equations (2.40) and (2.44), which give the system response $F^{-1}[T(j\omega)]$ for this case, probably are valid also, since the narrow-band equations derived from them have been shown to hold.

A filter which simulates the response of a conventional band-pass filter, but has a controllable -3 dB bandwidth may be realized by the N-path filter. A single pass-band response may be obtained from a filter having $N = 2$. If resistor R_1 in Figure 3.2 is replaced by a voltage-control

resistor, the effective Q and bandwidth of the filter may be varied by changing the resistor control voltage, thus changing the R-C time constant of the low-pass filter. The center frequency of the filter depends upon the sampling frequency, as usual, and may be adaptive or fixed. Such an adaptive bandwidth filter may be useful for intermediate-frequency filtering in communications equipment, or in very narrow-band wave analyzers or spectrum analyzers.

A possible application of the adaptive N-path filter is the measurement of very low signal/noise ratios. Conventional equipment cannot measure signal/noise ratios below about 0 dB². The N-path filter with modulating functions derived from the filter output can synchronize to signals at signal/noise ratios of about -30 dB. With a filter optimized for the application, signal/noise ratios much less than -30 dB might be measured without requiring an external reference signal.

Other potential applications are in seismic and sonar signal filtering. Application of the N-path filter at RF frequencies would require a higher frequency phase-locked loop, and high frequency transistors or FET's for the filter modulating switches. Operating the filter at frequencies of a few hundred MHz should be possible with a circuit based on standard high-frequency components.

Further investigation should include the analysis of

a transient model for the N-path filter and phase-locked loop system. A determination of the noise threshold performance would be desirable if the system is to be used as a signal demodulator.

REFERENCES

- [1] Franks, L. E. and I. W. Sandberg, "An Alternative Approach to the Realization of Network Transfer Functions: The N-Path Filter", Bell System Technical Journal, September, 1960.
- [2] Franks, L. E. and I. W. Sandberg, "An Alternative Approach to the Realization of Network Transfer Functions: The N-Path Filter", Bell System Technical Journal, September, 1960.
- [3] Gupta, S.C. and L. Hasdorff, "Fundamentals of Automatic Controls", John Wiley and Sons, Inc., New York, 1970.
- [4] Klapper, J. and J. T. Frankle, "Phase-Locked and Frequency-Feedback Systems; Principles and Techniques", Academic Press, New York.
- [5] Van Cleave, J. R., "Spectrum Processing Receivers for Telemetry Applications", IFT Journal, Vol. 1, Number 3, June, 1974.
- [6] Van Cleave, J. R., "Spectrum Processing Receivers for Telemetry Applications", IFT Journal, Vol. 1, Number 3, June 1974.
- [7] Viterbi, A. J., "Principles of Coherent Communications", McGraw-Hill, New York, 1966.
- [8] Zadeh, L. A. and C. A. Desoer, "Linear System Theory: The State Space Approach", McGraw-Hill, New York, 1963.

APPENDIX A

Demonstration of Matched Filter Property of the N-path Filter for Non-sinusoidal Signals

It can be shown that the frequency-modulated N-path filter may generate a matched-filter response for a periodic, non-sinusoidal, band-limited signal which may be frequency modulated.

Consider such a signal of fundamental frequency $\omega_0/2\pi$, band-limited to $N/2$ harmonics. A Fourier series of the following form can be written for the signal, $g(t)$:

$$g(t) = \sum_{p=1}^{p=N/2} C_p \cos(p\omega_0 t + \phi_p) \quad , \quad (A.1)$$

where C_p and ϕ are constants. Let the argument of the cosine function in equation (A.1) be frequency-modulated by a sinusoidal signal of frequency $\omega_s/2\pi$, and modulation index m , in a manner similar to that in the derivation of (2.40). The argument of the cosine function in the frequency-modulated case may be written as $p[\omega_0 t + m \sin(\omega_s t + \theta)] + \phi_p$, where ϕ_p is a constant. Equation (A.1) may be written for the frequency-modulated case as

$$g(t) = \sum_{p=1}^{p=N/2} C_p \cos[p\omega_0 t + \phi_p + pm \sin(\omega_s t + \theta)]. \quad (A.2)$$

Expanding the cosine function in (A.2) yields

$$\begin{aligned}
g(t) = & \sum_{p=1}^{p=N/2} C_p \{ \cos(p\omega_o t + \phi_p) \cos[pm \sin(\omega_s t + \theta)] \\
& - \sin(p\omega_o t + \phi_p) \sin[pm \sin(\omega_s t + \theta)] \}. \quad (A.3)
\end{aligned}$$

Expanding (A.3) using the Bessel function relationships, (2.41) - (2.43), it is seen that

$$\begin{aligned}
g(t) = & \sum_{p=1}^{p=N/2} C_p \{ \cos(p\omega_o t + \phi_p) [J_o(pm) \\
& + 2 \sum_{n=1}^{n=\infty} J_{2n}(pm) \cos 2n(\omega_s t + \theta) \\
& - \sin(p\omega_o t + \phi_p) [2 \sum_{n=0}^{n=\infty} J_{2n+1}(pm) \sin(2n+1)(\omega_s t + \theta)] \}. \quad (A.4)
\end{aligned}$$

The spectral components of the signal $g(t)$ are seen to occupy the same frequencies as the spectral components of the oscillatory part of the system response $F^{-1}[T(j\omega)]$ given by (2.40) for the frequency-modulated case. Therefore the spectral components of $g(t)$ coincide with the band-pass windows of $|T(j\omega)|$. Hence the system function $T(j\omega)$ for the N -path filter may match non-sinusoidal as well as sinusoidal, periodic, band-limited waveforms which may be frequency-modulated. It is this property which enables the N -path filter to recover waveforms of arbitrary shape,

which are subject to the band-limiting constraint above,
from wide-band noise.

APPENDIX B

Phase-Locked Loop Principles

A phase-locked loop is an automatic control system in which the controlled variable is phase. An elementary type 1 loop consists of three major components: a phase detector, a linear time-invariant filter, and a voltage controlled oscillator (VCO). A block diagram of a phase-locked loop is shown in Figure B.1. If a constant frequency signal within the lock range of the loop is applied to the input, a signal appears at the phase detector output and has a dc level which is proportional to the phase difference between the input signal and the reference signal produced by the VCO. After filtering, the dc component of the phase detector output signal is applied to the VCO control input and forces the VCO frequency to vary in a direction which reduces the phase difference between the input and the VCO signals. When the phase difference between input and VCO output signals is sufficiently small, the phase-locked loop synchronizes or "phase locks" to the input with a constant phase difference. The constant phase difference is necessary in a type 1 loop to generate the voltage required to shift the VCO frequency from the quiescent value to the frequency of the input signal. When the loop is locked, the phase detector output signal has a dc component which is always passed

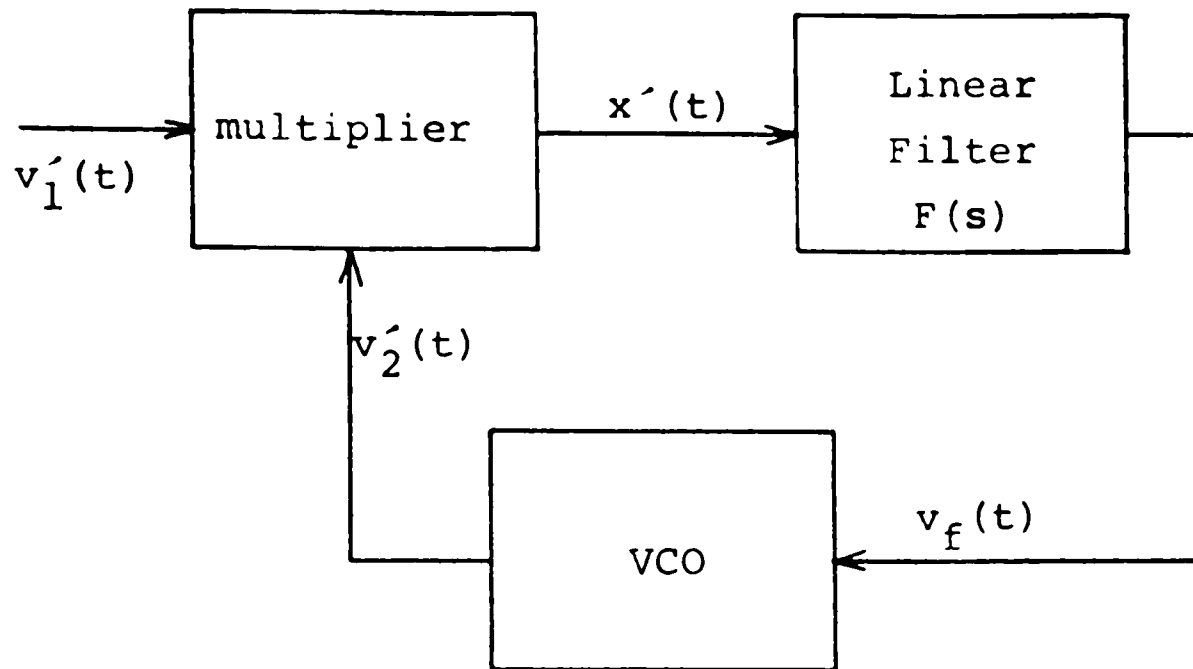


Figure B.1. Block diagram of elementary phase-locked loop.

by the loop low-pass filter. Hence the range of the frequencies over which the loop can remain locked is limited by the maximum output of the phase detector and the corresponding deviation of the VCO. The lock range is essentially a fixed parameter of the system, independent of the cutoff frequency of the low-pass filter.

Consider a phase-locked loop in which the phase detector is an analog multiplier. Let the input voltage be

$$v_1'(t) = \sqrt{2} K_1 \sin \theta_1(t) \quad . \quad (\text{B.1})$$

Let the VCO output signal be

$$v_1'(t) = \sqrt{2} K_2 \cos \theta_2(t) \quad , \quad (\text{B.2})$$

where K_1 and K_2 are constants. Denote the quiescent frequency of the VCO by $\omega_0/2\pi$. Then the VCO output angular frequency $\frac{d\theta'(t)}{dt}$ will be given by

$$\frac{d\theta'(t)}{dt} = \omega_0 + K_0 v_f(t) \quad , \quad (\text{B.3})$$

where K_0 is the VCO gain constant, having dimensions of rad/volt-second, and $v_f(t)$ is the VCO control voltage. The output of the multiplier is then given by the product of (B.1) and (B.2) and is

$$x(t) = K_1 K_2 \{ \sin[\theta(t) + \theta'(t)] + \sin[\theta(t) - \theta'(t)] \} . \quad (\text{B.4})$$

Since the low-pass filter eliminates the sum-frequency component, the following equivalent input to the filter may be written:

$$x'(t) = K_1 K_2 \sin[\theta(t) - \theta'(t)] . \quad (\text{B.5})$$

The low-pass filter is characterized by a transfer function, $F(s)$, and therefore an impulse response, $f(t)$. Convolution may be used to calculate the output of the filter, yielding

$$v_f(t) = \int_0^t f(t-u)x'(u)du . \quad (\text{B.6})$$

Substituting (B.5) and (B.6) into (B.3), the VCO output angular frequency can be written as

$$\frac{d\theta'(t)}{dt} = \omega_0 + K_0 \int_0^t f(t-u)K_1K_2 \sin[\theta(u) - \theta'(u)]du. \quad (\text{B.7})$$

Defining

$$\theta'_e(t) = \theta(t) - \theta'(t) , \quad (\text{B.8})$$

and

$$K = K_0 K_2 , \quad (\text{B.9})$$

(B.7) may be written as follows:

$$\frac{d\theta'_e(t)}{dt} = \frac{d\theta(t)}{dt} - \omega_o - K_1 K \int_0^t f(t-u) \sin\theta'_e(u) du. \quad (\text{B.10})$$

Equation (B.10) evidently describes the exact behavior of the phase-locked loop for a noise-free, sinusoidal input. Solutions to this equation have been obtained for loops containing no filter, and loops containing ideal integrators [5,6]. However, a linearized model and the classes of inputs for which linearization is justified are of primary importance.

The Linear Model

Making the following substitutions to normalize the loop variables,

$$\theta_i(t) = \theta(t) - \omega_o t, \quad (\text{B.11})$$

$$\theta_o(t) = \theta'(t) - \omega_o, \quad (\text{B.12})$$

and
$$\theta_e(t) = \theta'_e(t) - \omega_o, \quad (\text{B.13})$$

(B.10) becomes

$$\frac{d\theta_e(t)}{dt} = \frac{d\theta_i(t)}{dt} - K_1 K \int_0^t f(t-u) \sin\theta'_e(u) du, \quad (\text{B.14})$$

which leads directly to the model of Figure B.2. The VCO has been replaced by an ideal integrator; the multiplier

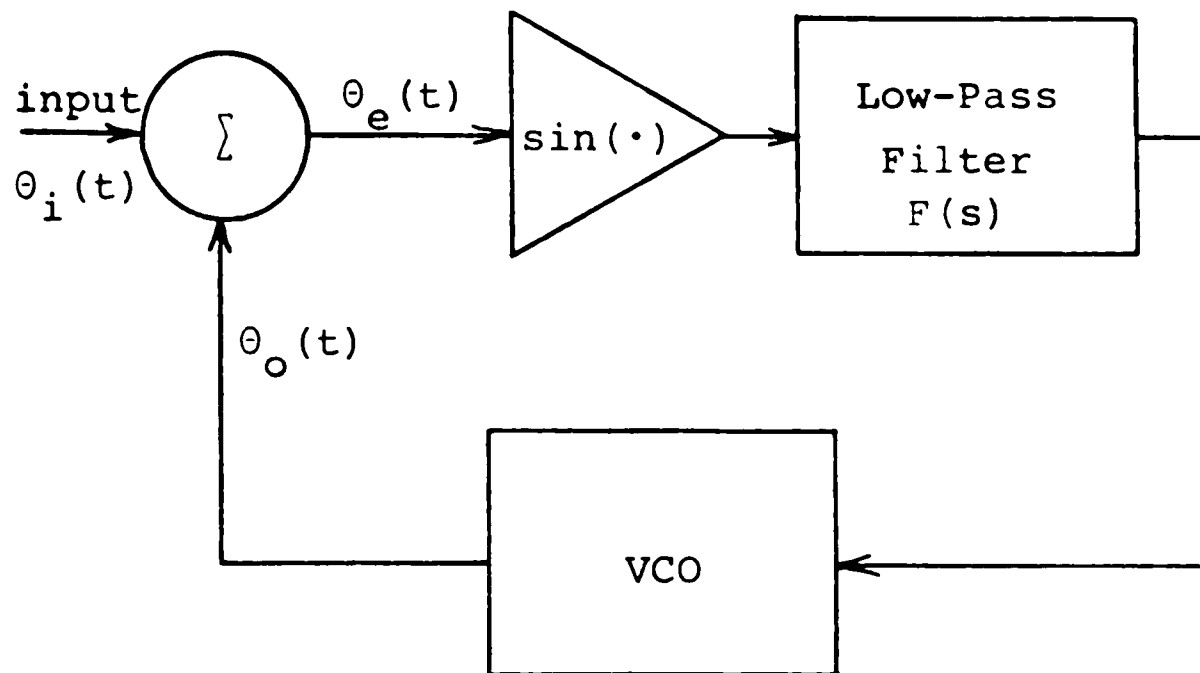


Figure B.2. Model of phase-locked loop

by a subtractor and a nonlinear element. The controlled variable is now phase.

Since the phase-locked loop is used to generate a filter modulating function which is coherent with the loop input, the phase error, $\theta_e(t)$, is required to be very small (or zero) under steady state conditions. Since $\sin\theta_e(t) \approx \theta_e(t)$ for small $\theta_e(t)$, the nonlinearity can be dropped from (B.14), giving

$$\frac{d\theta_i(t)}{dt} = \frac{d\theta_e(t)}{dt} + K_1 K \int_0^t f(t-u)\theta_e(u)du . \quad (\text{B.15})$$

It is assumed that the loop filter can be characterized by a transfer function, $F(s)$. If the Laplace transform of (B.15) is found, it is seen that

$$s\theta_i(s) = s\theta_e(s) + K_1 K F(s)\theta_e(s) ,$$

thus

$$\theta_e(s) = \left[\frac{1}{1 + K_1 K F(s)/s} \right] \theta_i(s) , \quad (\text{B.16})$$

and

$$\theta_o(s) = \left[\frac{K_1 K F(s)/s}{1 + K_1 K F(s)/s} \right] \theta_i(s) . \quad (\text{B.17})$$

The term multiplying $\theta_i(s)$ in (B.17) is called the "closed loop transfer function", $H(s)$. The polynomial equation $1 + K_1 K F(s)/s = 0$ is denoted by the "characteristic

equation" of $H(s)$. The roots of the characteristic equation determine the poles of the closed-loop transfer function. The system "type" is the number of poles of the polynomial $K_1 K F(s)/s$ located at the origin. The system type, then, corresponds to the number of pure integrators in the loop. The "order" of the system is the degree of the highest ordered term in the characteristic equation. Standard techniques developed in control systems texts may be applied to (B.16) and (B.17) to find the transient and steady-state performance of the phase-locked loop system [7,8].

